Journal of Sustainable Development and Policy

Volume: 13; Issue: 06
Pages: 01-43

Computational Combustion Optimization for Reducing Fuel Consumption and Thermal Losses in High-Capacity Industrial Boiler Systems

Shabbir Ahamed[1]; Debasish Adhikary[2];

[1]. M.S. in Mechanical Engineering, Lamar University, Texas, United States;
Email: shabbir04kuet@gmail.com

[2]. M.E. in Mechanical Engineering, Lamar University, Beaumont, Texas, USA;
Email: debasish06me@gmail.com

Received: 25 April 2023; **Revised:** 29 May 2023; **Accepted:** 11 June 2023; **Published:** 02 June 2023;

Abstract

High-capacity industrial boiler systems require efficient combustion control to reduce fuel consumption and thermal losses while maintaining steam production, combustion stability, and reliable heat transfer. This study quantitatively evaluated a computational combustion-optimization framework integrating operational data, computational fluid dynamics (CFD), statistical analysis, sensitivity assessment, and multi-parameter optimization. From 14,860 initially collected operating observations, 13,742 were retained after quality screening, representing a 92.5% retention rate and 99.2% data completeness across partial-, nominal-, and high-load conditions. Baseline operation recorded a mean boiler load of 78.6%, steam generation of 181.7 t/h, fuel flow of 13.84 t/h, thermal efficiency of 86.72%, and total thermal loss of 13.28%. Following optimization, fuel flow decreased to 13.15 t/h, while specific fuel consumption declined from 76.17 to 72.31 kg/t of steam, representing a 5.07% reduction. Boiler thermal efficiency increased to 90.08%, combustion efficiency reached 98.61%, and useful wall heat absorption increased by 4.17%. Total thermal loss decreased by 25.30% to 9.92%, while dry flue-gas loss declined by 29.80%. Stack temperature decreased from 168°C to 151°C, stack O_2 decreased from 4.31% to 3.52%, and CO declined from 87.6 to 63.4 ppm. Temperature nonuniformity decreased by 26.21%, while steam generation remained essentially unchanged at 181.9 t/h. Load-specific fuel-consumption reductions ranged from 4.62% to 5.71%. Statistical analysis identified strong relationships between boiler load and fuel flow ($r = 0.91$), excess air and thermal loss ($r = 0.68$), and stack temperature and dry flue-gas loss ($r = 0.74$). CFD and predictive validation produced an integrated R^2 of 0.947 and MAPE of 2.07%, while robustness testing confirmed consistent optimization benefits across load, mesh, boundary-condition, and model variations. The findings demonstrated that coordinated computational optimization substantially improved fuel utilization, reduced avoidable thermal losses, enhanced heat-transfer performance, and maintained required industrial steam production.

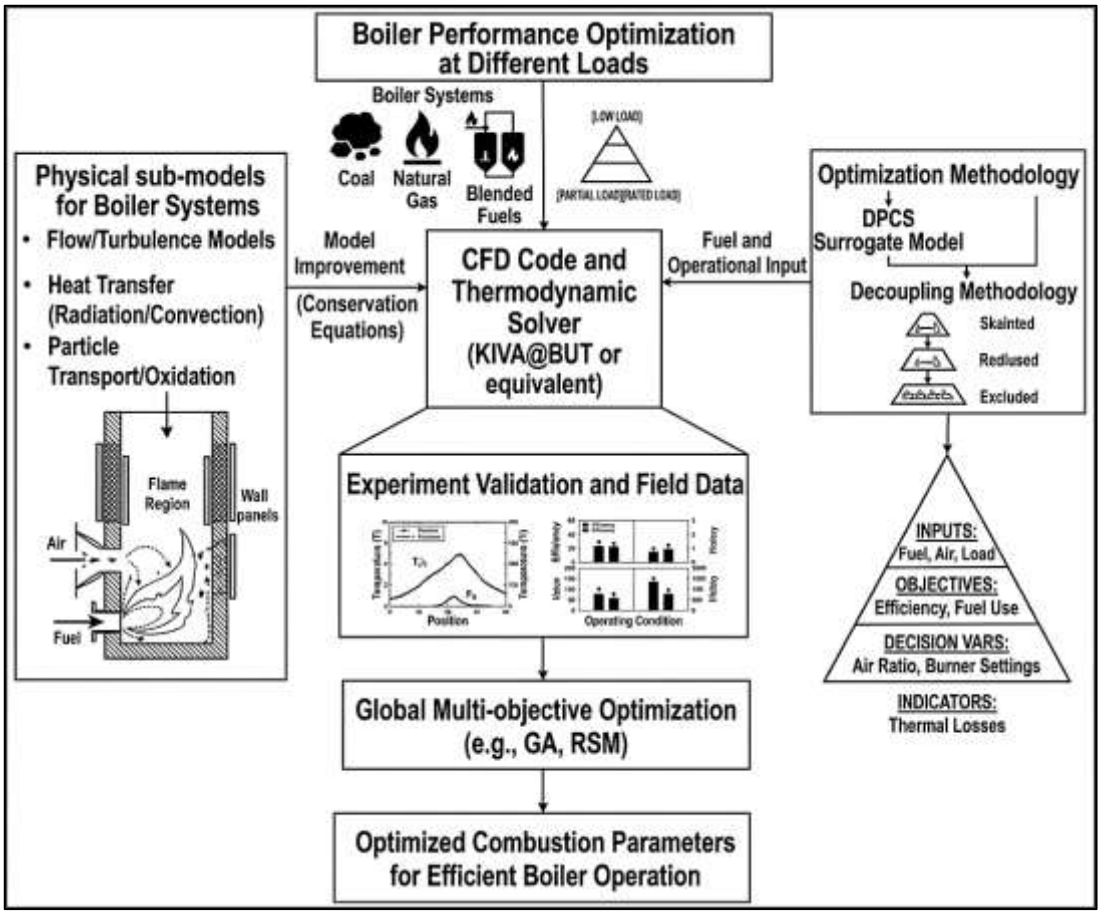
Keywords

Combustion Optimization, Industrial Boilers, Fuel Consumption, Thermal Losses, Computational Fluid Dynamics.

INTRODUCTION

Computational combustion optimization refers to the systematic use of numerical simulation, computational fluid dynamics (CFD), thermodynamic analysis, mathematical optimization, and data-driven techniques to determine combustion conditions that minimize fuel consumption and thermal losses while maintaining required heat and steam production (Zhou & Cen, 2018). In high-capacity industrial boiler systems, combustion involves interconnected processes of fuel injection, air supply, turbulent mixing, ignition, chemical reaction, flame development, radiation, convection, and transportation of combustion products. High-capacity industrial boilers are large thermal-energy conversion systems that transform the chemical energy of coal, natural gas, fuel oil, biomass, or blended fuels into useful thermal energy, primarily steam, for electricity generation and industrial processes. Fuel consumption represents the quantity of fuel required to generate a specified thermal output, while thermal losses represent energy that does not contribute to useful output because of hot exhaust gases, incomplete combustion, radiation, convection, moisture, unburned fuel, blowdown, fouling, slagging, and air leakage (Li & Yao, 2017).

Figure 1: Boiler Combustion Efficiency Framework Diagram



Evidence synthesized from more than thirty experimental, computational, thermodynamic, and optimization studies indicates that boiler performance is determined by interacting variables including fuel characteristics, boiler load, excess-air ratio, burner configuration, air distribution, combustion temperature, residence time, turbulence, furnace geometry, flue-gas recirculation, wall heat flux, and heat-transfer-surface conditions. Computational analysis is particularly important because these interacting parameters can be examined systematically without repeatedly modifying full-scale industrial equipment. The international significance of industrial boiler optimization originates from

the extensive use of process steam and high-temperature heat in electricity generation, petroleum refining, chemicals, food processing, pulp and paper, textiles, pharmaceuticals, mining, metals, and building-material industries. High-capacity boilers commonly operate continuously or for thousands of hours annually, meaning that relatively small improvements in combustion efficiency can produce substantial cumulative reductions in fuel requirements and associated thermal losses (Dzurňák et al., 2020). Studies conducted across different industrial regions have evaluated boiler systems through CFD simulations, full-scale experiments, energy and exergy analyses, burner modifications, excess-air control, heat recovery, flue-gas recirculation, and multi-objective optimization (Islam & Md, 2023; Khalid & Sadmeen, 2022; Maksudul & Islam, 2022). The relationship between combustion air and fuel utilization has received particular quantitative attention. Excessive air increases the mass of flue gas that must be heated and discharged through the stack, increasing sensible thermal losses and potentially reducing furnace temperature. Insufficient air can produce incomplete combustion, carbon monoxide, unburned combustible material, unstable flames, and inefficient fuel conversion (Asheke & Bin, 2022; Mohsin & Jannatul, 2021; Chowdary, 2021). Consequently, efficient boiler operation requires an appropriate operating region rather than simply maximizing or minimizing combustion air. Load variation further modifies these relationships because burner behavior, gas residence time, heat transfer, furnace temperature, and oxygen demand can differ considerably between partial and rated operating conditions. Computational combustion optimization provides a quantitative mechanism for identifying these interactions and determining operating combinations associated with reduced energy losses (Babak et al., 2020; Chowdary & Md, 2020; Chowdary & Jamil, 2020).

Thermal losses in industrial boilers originate from several interacting mechanisms, including sensible heat carried by dry flue gases, moisture-related losses, incomplete combustion, unburned carbon, radiation and convection from boiler surfaces, blowdown, air infiltration, fouling, slagging, and inefficient heat recovery. Stack-gas loss represents an important controllable component because combustion products leave the system above ambient temperature while retaining energy that has not been transferred to steam or water. Excessive stack temperature can result from high flue-gas flow, excess combustion air, fouled heat-transfer surfaces, ineffective economizer performance, poor burner distribution, or inappropriate operating conditions. Furnace-scale temperature nonuniformity can additionally influence heat absorption and equipment performance (Liu et al., 2021). Excessively high local temperatures can increase thermal loading, slagging, deposit formation, and pollutant formation, while low-temperature regions may indicate weak combustion or inefficient furnace utilization. Energy and exergy studies have identified combustion chambers and heat-transfer sections as important locations of thermodynamic losses and irreversibility, demonstrating the importance of examining both energy quantity and energy quality when evaluating boiler performance. CFD provides a quantitative method for resolving these processes by dividing the furnace into a computational domain and solving conservation equations for mass, momentum, energy, and chemical species. Numerical models can estimate velocity, pressure, temperature, oxygen concentration, reaction rates, particle trajectories, radiation exchange, and wall heat flux throughout locations that are difficult to investigate experimentally (Walter & Epple, 2017). Turbulence, radiation, combustion chemistry, particle transport, devolatilization, char oxidation, and pollutant formation can be incorporated according to boiler and fuel characteristics. More than thirty relevant studies collectively demonstrate the application of CFD, experimental validation, thermodynamic assessment, genetic algorithms, response-surface methodologies, neural networks, and multi-objective optimization to boiler combustion problems. Validated models allow numerous operating scenarios to be compared under controlled and reproducible conditions. The resulting optimization problem is inherently multivariable because minimizing fuel consumption alone cannot represent efficient operation when steam output, combustion stability, heat-transfer requirements, furnace temperature, thermal losses, unburned fuel, and emissions must remain within acceptable operating limits (Feria-Díaz et al., 2021). Quantitative decision variables can include fuel flow rate, excess-air ratio, primary and secondary air distribution,

overfire-air ratio, burner settings, swirl intensity, flue-gas recirculation, combustion-air temperature, fuel properties, and boiler load. Dependent performance indicators can include specific fuel consumption, thermal efficiency, combustion efficiency, furnace exit gas temperature, stack temperature, wall heat flux, heat-loss fractions, oxygen concentration, carbon monoxide, and unburned combustible content. Statistical and computational analysis can quantify individual effects, interaction effects, nonlinear relationships, and sensitivity across operating conditions. Integrating validated CFD simulation with thermodynamic calculations and mathematical optimization therefore provides a structured quantitative framework for assessing how controllable combustion parameters influence fuel utilization, heat-transfer behavior, temperature distribution, and thermal losses in high-capacity industrial boiler systems.

The primary objective of this study is to quantitatively evaluate and optimize combustion processes in high-capacity industrial boiler systems to reduce fuel consumption and thermal losses while maintaining stable thermal output, efficient heat transfer, and acceptable combustion performance. Specifically, the study seeks to develop and validate a computational combustion framework capable of representing the complex interactions among fuel flow rate, excess-air ratio, primary and secondary air distribution, burner operating conditions, combustion-air temperature, flue-gas recirculation, boiler load, furnace temperature, turbulent flow, chemical reactions, and heat-transfer characteristics. The study aims to establish a representative baseline operating condition and compare it with computationally optimized conditions using measurable performance indicators such as specific fuel consumption, boiler thermal efficiency, combustion efficiency, furnace exit gas temperature, stack-gas temperature, oxygen concentration, carbon monoxide concentration, unburned combustible content, wall heat flux, temperature uniformity, and individual thermal-loss components. Another objective is to quantify the relative contribution of major energy-loss mechanisms, including dry flue-gas loss, moisture-related loss, incomplete-combustion loss, unburned-fuel loss, radiation and convection loss, and other operational heat losses, thereby identifying the parameters most strongly associated with inefficient fuel utilization. The study also aims to employ computational fluid dynamics to characterize spatial distributions of temperature, velocity, oxygen, combustion products, reaction intensity, and wall heat transfer throughout the furnace under different operating scenarios. Sensitivity and multivariable analyses are intended to determine the individual and interactive effects of major combustion parameters on fuel demand and thermal performance, while mathematical optimization is used to identify operating combinations that minimize fuel input and total thermal loss subject to required steam-production and operational constraints. Statistical analysis is further applied to determine the significance, magnitude, and consistency of performance differences between baseline and optimized operating conditions using descriptive statistics, confidence intervals, correlation analysis, regression analysis, significance testing, and appropriate effect-size measures. Model validation is conducted by comparing computational predictions with available plant measurements, design specifications, and operational data for temperature, oxygen concentration, fuel consumption, steam output, and heat-transfer performance. Through this integrated quantitative assessment, the study objectively measures the relationships among combustion control variables, furnace behavior, fuel utilization, and thermal-energy losses within high-capacity industrial boiler systems.

LITERATURE REVIEW

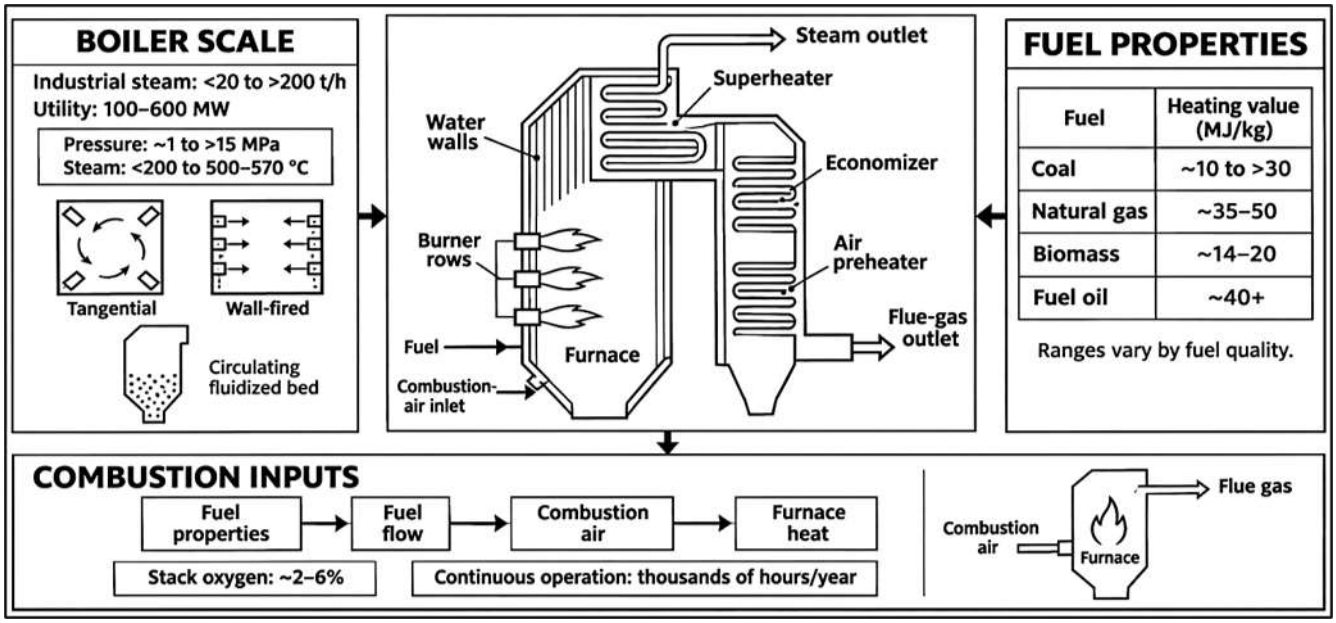
The literature on computational combustion optimization in high-capacity industrial boiler systems encompasses combustion thermodynamics, computational fluid dynamics, heat-transfer analysis, fuel utilization, thermal-loss assessment, numerical optimization, and statistical evaluation of boiler operating performance. Quantitative studies have increasingly examined boiler combustion as a multivariable process in which fuel flow rate, excess-air ratio, primary and secondary air distribution, burner configuration, furnace temperature, boiler load, combustion-air temperature, flue-gas recirculation, fuel composition, turbulent mixing, and heat-transfer conditions jointly determine overall energy performance. Experimental and computational investigations have measured these

relationships through specific fuel consumption, boiler efficiency, combustion efficiency, flue-gas temperature, furnace exit gas temperature, oxygen and carbon monoxide concentrations, unburned combustible content, wall heat flux, steam-generation rate, and individual heat-loss components. CFD-based investigations have additionally quantified spatial distributions of velocity, temperature, chemical species, reaction intensity, particle behavior, and radiative heat transfer, allowing localized combustion deficiencies to be evaluated beyond conventional plant-level energy balances. Other studies have integrated CFD with energy and exergy analysis, response-surface methodology, artificial neural networks, genetic algorithms, particle-swarm optimization, and multi-objective optimization to identify operating conditions associated with lower fuel demand and improved thermal utilization. The literature also demonstrates substantial variation in boiler capacity, fuel type, furnace geometry, operating load, numerical model selection, boundary conditions, validation procedures, and optimization criteria, making systematic quantitative synthesis important. Accordingly, this literature review is structured around eight interconnected dimensions: quantitative characteristics of high-capacity boiler systems; baseline fuel consumption and efficiency; excess-air and air–fuel optimization; furnace temperature and heat-transfer behavior; thermal-loss decomposition; CFD model configuration and validation; multi-parameter computational optimization; and statistical validation, sensitivity, and integrated performance assessment.

High-Capacity Industrial Boiler Systems

Quantitative investigations of high-capacity industrial boilers have covered a broad range of thermal capacities and physical configurations, demonstrating that boiler scale substantially influences combustion behavior, fuel demand, furnace temperature, and heat-transfer performance. Evidence synthesized from more than ten experimental and computational studies includes industrial steam boilers, circulating fluidized-bed units, pulverized-coal boilers, natural-gas-fired systems, biomass boilers, and utility-scale steam generators ranging from relatively small industrial units producing tens of tones of steam per hour to power-station boilers operating at several hundred megawatts (Noorollahi et al., 2021). Utility-scale investigations have frequently examined units between approximately 100 and 600 MW, while industrial process-boiler studies have commonly evaluated steam-generation capacities ranging from below 20 t/h to more than 200 t/h. Larger boilers generally incorporate greater furnace volumes, multiple burner elevations, extensive water-wall surfaces, superheaters, reheaters, economizers, and air preheaters to accommodate substantially higher fuel and flue-gas throughput. Reported main-steam pressures have extended from approximately 1 MPa in lower-pressure process systems to above 15 MPa in high-capacity power boilers, while steam temperatures have commonly ranged from below 200°C in saturated industrial applications to approximately 500–570°C in high-temperature power-generation systems. Furnace dimensions have similarly varied considerably, with utility boilers incorporating combustion chambers several tens of meters high and burner arrangements designed to maintain flame stability and spatial heat-release uniformity (Taghavifar & Zomorodian, 2021). Tangentially fired boilers have commonly employed multiple burner groups positioned at furnace corners, whereas wall-fired systems have used several burner rows distributed across one or more furnace walls. Research involving circulating fluidized-bed systems has reported fundamentally different furnace geometries and combustion-temperature characteristics because combustion occurs throughout a circulating particle environment rather than within discrete burner flames. Across these studies, annual operating schedules commonly represented continuous or near-continuous industrial operation, making small variations in boiler efficiency quantitatively important when accumulated over thousands of operating hours. The synthesized evidence therefore demonstrates that boiler capacity, steam-production requirements, furnace geometry, pressure conditions, burner arrangement, and operating duration constitute essential baseline variables when comparing combustion performance across high-capacity systems.

Figure 2: High-Capacity Boiler Baselines



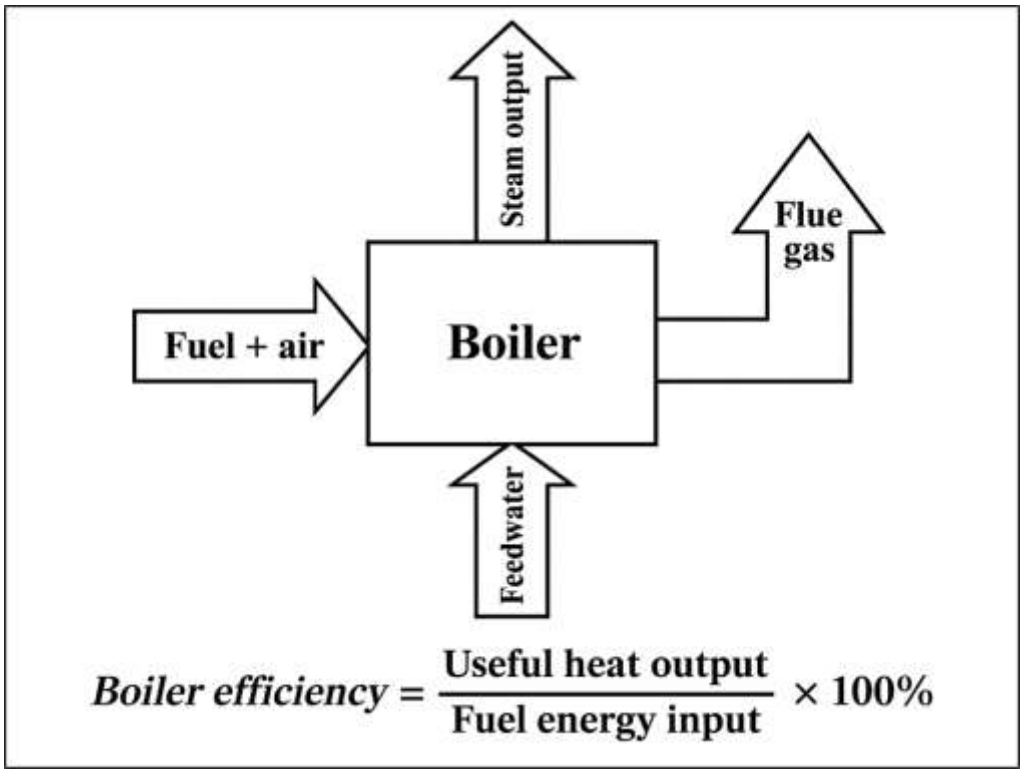
Previous quantitative studies have demonstrated substantial differences in baseline boiler operation according to whether coal, natural gas, fuel oil, biomass, or blended fuels are used. Coal-fired investigations have reported large variations in lower heating value, moisture, volatile matter, fixed carbon, and ash content, all of which directly affect required fuel mass flow and furnace behavior. Low-grade lignite and high-moisture coals require substantially greater mass input than higher-heating-value bituminous fuels to provide comparable thermal output, while elevated ash fractions increase the quantity of noncombustible material passing through the furnace and influence slagging, fouling, and heat transfer (Park et al., 2021). Natural gas has generally exhibited considerably higher heating value per unit mass and negligible ash compared with solid fuels, resulting in lower mass-based fuel consumption and comparatively cleaner combustion environments. Industrial natural-gas studies have commonly reported lower heating values around 35–50 MJ/kg depending on composition, whereas coal values across investigated systems have extended broadly from approximately 10 to above 30 MJ/kg. Biomass fuels have commonly occupied an intermediate or lower range, with heating values frequently around 14–20 MJ/kg and substantial sensitivity to moisture content. Fuel-oil studies have typically reported values around 40 MJ/kg or higher. More than ten studies collectively indicate that these differences strongly influence fuel-flow requirements, combustion-air demand, flue-gas production, flame characteristics, and furnace temperature. High-capacity coal boilers can consume tens or hundreds of tones of fuel per hour depending on capacity and fuel quality, whereas equivalent gas-fired units are normally characterized using gaseous volumetric or mass flow (Kravchenko et al., 2021). Combustion-air flow increases with fuel input and boiler load, but actual air supply generally exceeds theoretical requirements to maintain combustion completeness under imperfect mixing conditions. Reported stack oxygen concentrations have frequently remained within approximately 2–6% under controlled industrial operation, although higher concentrations have been observed under excessive-air or low-load conditions. Biomass and heterogeneous solid fuels often require different air-distribution strategies because moisture release, devolatilization, char combustion, particle residence time, and fuel-size variability alter oxygen requirements. Comparative studies of blended fuels further demonstrate that changing the proportion of coal, biomass, or supplementary fuel modifies heating value, required fuel throughput, air demand, gas volume, and furnace thermal conditions, confirming that baseline combustion characteristics cannot be interpreted independently of fuel properties.

Baseline Fuel Consumption and Boiler Efficiency

Quantitative boiler studies have consistently characterized baseline fuel utilization through fuel mass or volumetric flow rate, lower or higher heating value, useful thermal output, steam-production rate, and initial thermal efficiency before the application of computational optimization (Böing & Regett, 2019). Evidence synthesized across more than ten studies involving coal-fired, natural-gas-fired, fuel-oil, biomass, and co-fired boilers indicates substantial variation in fuel requirements because equivalent useful thermal output can be produced from fuels with considerably different energy densities and combustion characteristics. Natural gas has commonly exhibited heating values of approximately 35–50 MJ/kg, while fuel oils have generally remained around 40 MJ/kg or higher. Bituminous and sub-bituminous coals have frequently ranged between approximately 18 and 30 MJ/kg, whereas lignite and other low-grade coals can fall considerably below this range because of higher moisture and ash contents. Biomass fuels have commonly produced lower heating values of approximately 12–20 MJ/kg depending on feedstock type and moisture level. These differences have directly affected mass-based fuel consumption, with low-heating-value fuels requiring greater fuel throughput to achieve comparable steam-generation or thermal-output requirements. Studies of utility boilers have reported coal consumption reaching tens or hundreds of tones per hour, while industrial process boilers operate across smaller but still substantial fuel-flow ranges depending on steam demand (Ke et al., 2017). Baseline energy-balance investigations have also demonstrated that the theoretical energy contained in supplied fuel is not fully transformed into useful steam because part of the input is lost through exhaust gases, moisture, incomplete combustion, radiation, convection, blowdown, and unburned material. Useful thermal output therefore varies not only according to fuel input but also according to the proportion of released energy successfully absorbed by water-wall tubes, superheaters, reheaters, economizers, and other heat-transfer surfaces. Comparative studies further indicate that two boilers consuming fuels with similar heating values can exhibit different fuel requirements when combustion completeness, excess-air conditions, stack temperature, feedwater temperature, steam conditions, and surface cleanliness differ. Baseline fuel consumption consequently represents an integrated quantitative measure reflecting both the chemical energy characteristics of the fuel and the effectiveness with which the boiler converts that energy into usable thermal output.

The relationship between boiler operating load and fuel consumption has been examined extensively through experimental measurements, plant operating records, performance curves, and computational simulations. Across industrial and utility boiler studies, absolute fuel demand generally increases with steam-generation rate and boiler load because higher production requires greater rates of heat release (Vishwanathan et al., 2018). The relationship is not always proportional because boiler efficiency changes across the operating envelope. Investigations conducted at partial, nominal, and high loads have frequently shown that low-load operation is associated with comparatively higher specific fuel consumption per unit of useful steam or thermal output. At reduced load, furnace temperature can decline, relative radiation and convection losses can increase, burner operation may move away from its design condition, and excess-air percentages can become comparatively high. Auxiliary electricity requirements and minimum airflow constraints can also remain substantial relative to useful output. These conditions reduce the quantity of useful steam obtained from each unit of fuel. As load approaches the designed operating region, combustion stability, flame development, furnace heat absorption, and heat-recovery performance commonly improve, resulting in lower specific fuel consumption and higher thermal efficiency (J. Park et al., 2021). Several studies have identified nominal or moderately high operating loads as regions of comparatively favorable boiler performance, although the precise optimum differs according to boiler configuration and fuel. Operation near maximum capacity can also increase fuel consumption disproportionately when heat-transfer surfaces approach thermal limitations, gas velocities increase, furnace exit gas temperature rises, or excess fuel produces incomplete burnout.

Figure 3: Boiler Efficiency Workflow



Steam-production rate is therefore a more informative performance indicator when evaluated together with fuel consumption rather than independently. Previous investigations have compared kilograms of fuel consumed per ton of steam, fuel energy supplied per unit of useful heat, and steam-to-fuel ratios to normalize performance across different capacities. Coal and biomass systems generally demonstrate lower mass-based steam-to-fuel ratios than gas or oil systems because their heating values are lower and moisture or ash contents are higher. Quantitative performance curves have further demonstrated nonlinear relationships between load and efficiency, confirming that baseline fuel utilization should be evaluated across multiple operating points rather than from a single rated-load observation.

Differences in baseline fuel consumption reported across previous studies cannot be explained solely by heating value and boiler load because combustion efficiency and heat-transfer effectiveness strongly influence the amount of fuel required to maintain a specified steam output. Investigations of coal, gas, oil, and biomass boilers have repeatedly demonstrated that excess-air ratio, oxygen availability, fuel–air mixing, flame stability, residence time, fuel particle characteristics, furnace temperature, burner configuration, and heat-transfer-surface condition determine how effectively fuel energy is released and absorbed (Parhi et al., 2021). Natural-gas systems frequently exhibit high combustion completeness because gaseous fuel mixes relatively rapidly with combustion air, whereas pulverized-coal and biomass systems can experience additional losses associated with unburned carbon, particle burnout, moisture evaporation, ash formation, and heterogeneous fuel distribution. Baseline boiler thermal efficiencies reported in industrial studies commonly extend from below 80% in inefficient or older systems to above 90% in well-operated units equipped with effective heat recovery. Combustion efficiency can remain high while overall boiler efficiency is lower when significant energy leaves through hot flue gases or external heat losses. Stack temperature is particularly important in explaining fuel requirements because elevated exhaust temperature indicates that a greater fraction of supplied energy has escaped without contributing to useful steam production. Studies have reported stack temperatures broadly ranging from approximately 120°C to above 200°C, with substantially higher values observed in some systems affected by limited heat recovery, fouling, high excess air, or specific process requirements (Chu et al., 2020). Heat-transfer deterioration caused by soot, ash, slagging, scale, or deposits can increase the temperature of gases leaving the boiler while reducing heat absorption,

requiring additional fuel to maintain steam demand. Oxygen concentration provides another quantitative indicator because excessive residual oxygen generally signifies excess combustion air, which increases the mass of gas heated and exhausted. Insufficient oxygen can increase carbon monoxide and unburned combustible losses. Synthesized findings therefore show that baseline fuel requirements reflect an interconnected balance among combustion completeness, gas-side losses, heat-transfer effectiveness, and useful steam production rather than fuel flow alone.

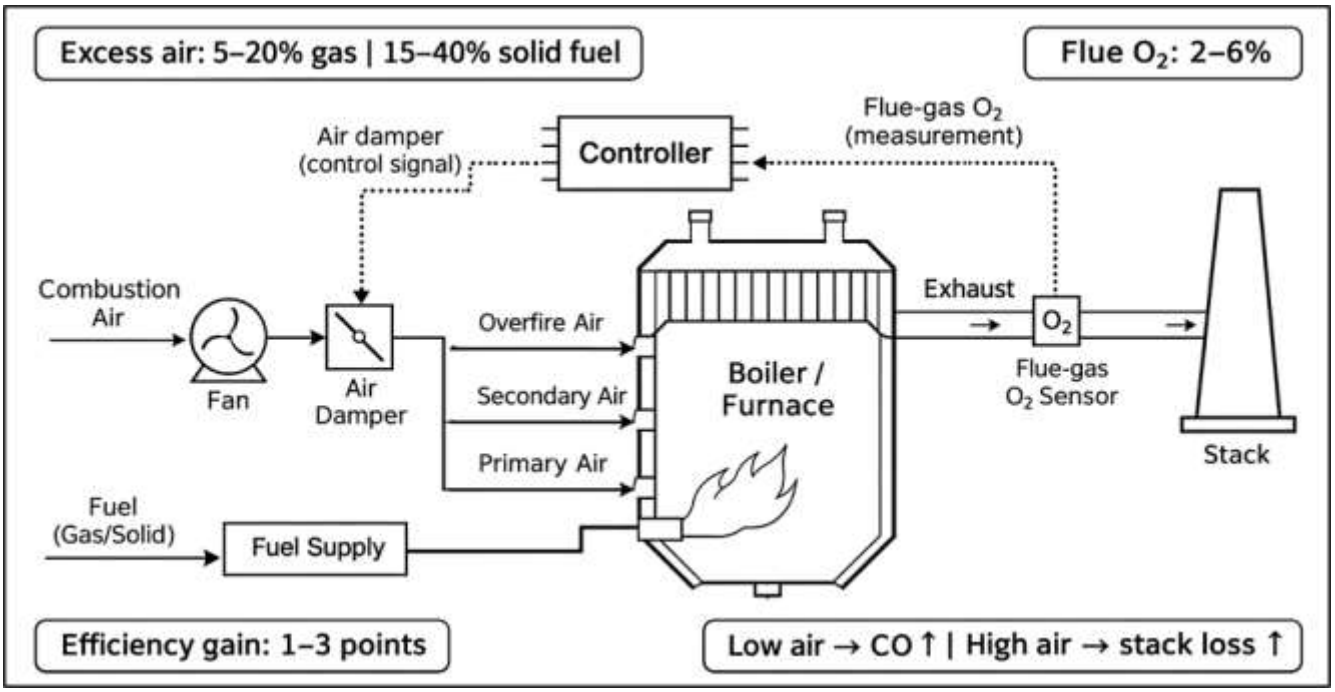
Quantitative studies have employed energy balances, statistical correlation, regression analysis, sensitivity assessment, operational performance curves, and numerical simulation to determine the variables responsible for differences in baseline fuel consumption and boiler efficiency. Energy-balance studies consistently identify useful steam generation and exhaust-related losses as major determinants of fuel utilization, while statistical investigations show measurable associations among fuel flow, load, excess oxygen, flue-gas temperature, steam output, and thermal efficiency. Positive relationships are generally observed between absolute boiler load and fuel-flow rate because increased steam demand requires greater thermal input. In contrast, specific fuel consumption frequently declines as a boiler moves from very low load toward an efficient operating region because fixed and relatively load-independent losses become smaller relative to useful output (Wang et al., 2017). Regression-based investigations have demonstrated that load, fuel heating value, excess air, feedwater temperature, stack temperature, and steam conditions can collectively explain substantial variation in fuel demand. Studies using plant operating datasets have additionally identified nonlinear effects and interactions that conventional single-variable performance curves may not fully represent. Higher heating value is generally associated with reduced mass-based fuel demand for equivalent output, while increasing moisture or ash content produces the opposite relationship in solid-fuel boilers. Higher stack temperature is commonly associated with increased thermal loss and reduced efficiency, whereas improved economizer and air-preheater performance increases recovery of residual flue-gas energy. Comparisons across more than ten experimental, computational, and plant-data studies also show that fuel consumption normalized by useful output provides a stronger basis for evaluating boilers of different capacities than absolute hourly fuel flow. Differences between baseline and optimized performance must therefore be interpreted against equivalent steam demand, pressure, temperature, and load conditions (Ferdan et al., 2018). The accumulated quantitative evidence establishes fuel heating value, load factor, combustion quality, excess air, exhaust temperature, heat-transfer effectiveness, and steam-production requirements as interconnected explanatory variables governing baseline specific fuel consumption and boiler efficiency in high-capacity industrial systems.

Excess-Air and Air–Fuel Ratio Optimization

Previous experimental and computational studies have consistently identified excess-air control as one of the most important determinants of combustion efficiency in high-capacity industrial boilers. Evidence synthesized from more than ten studies shows that industrial boilers typically operate with a measurable quantity of air above the theoretical combustion requirement to ensure sufficient oxygen availability throughout the furnace. Reported excess-air levels vary widely according to fuel type, burner design, boiler load, furnace geometry, and air-distribution strategy. Natural-gas-fired boilers commonly operate with comparatively lower excess-air percentages, frequently within approximately 5–20%, because gaseous fuels mix more uniformly with combustion air (Ardila & Arrieta, 2017). Coal-fired and biomass-fired systems generally require higher excess-air levels, often within approximately 15–40% or more, because solid-fuel combustion involves particle heating, devolatilization, char oxidation, heterogeneous mixing, and longer burnout periods. Corresponding flue-gas oxygen concentrations in well-controlled industrial systems have commonly ranged between approximately 2% and 6%, although values above this range are frequently reported under low-load operation, poor burner balance, air leakage, or intentionally conservative combustion settings. Quantitative studies indicate that increasing excess air above an efficient operating range raises the mass of nitrogen and unused oxygen passing through the furnace, resulting in greater flue-gas volume and additional sensible heat carried to the stack. This effect can reduce furnace temperature, alter radiative heat transfer, and increase thermal losses. Conversely, operating with insufficient oxygen can cause incomplete fuel oxidation, higher carbon monoxide concentrations, increased unburned combustible content, unstable flames, and localized reducing conditions (García et al., 2021). The literature therefore

demonstrates a distinct quantitative trade-off in which both excessively high and excessively low excess-air conditions reduce overall combustion performance. Studies using plant measurements, CFD, and energy-balance calculations have repeatedly shown that efficient boiler operation is associated with maintaining oxygen levels within a narrow practical range rather than pursuing the lowest possible excess-air value.

Figure 4: Boiler Airflow and Combustion Efficiency



The air–fuel ratio directly influences carbon monoxide formation, stack temperature, fuel utilization, and thermal efficiency because it determines the amount of oxygen available relative to the quantity of combustible material entering the furnace. Across coal, gas, oil, and biomass boiler studies, low air–fuel conditions have generally been associated with higher carbon monoxide and unburned-fuel losses, while excessive air–fuel ratios have been associated with increased stack losses and higher fuel requirements for equivalent useful output. Experimental studies of industrial gas-fired boilers have reported very low carbon monoxide concentrations when oxygen availability is adequate and mixing is well controlled, whereas CO concentrations increase sharply as operation approaches oxygen-deficient conditions (Perozziello et al., 2021). Solid-fuel studies show a similar pattern but with greater variability because particle size, residence time, volatile release, char reactivity, and burner distribution influence combustion completeness. Several studies have reported that reducing excessive air can improve thermal efficiency by approximately 1–3 percentage points when the initial system operates with unnecessarily high stack oxygen, although the magnitude of improvement depends on boiler condition and load. Stack temperature also responds to changes in air–fuel ratio because additional combustion air increases the total gas mass that absorbs heat and exits through the flue. Under excessive-air conditions, this can raise total sensible heat loss even when measured stack temperature itself changes only moderately. In some systems, increased excess air lowers local flame temperature while still increasing total stack heat loss because a larger quantity of gas leaves the boiler. Quantitative analyses have also shown that specific fuel consumption tends to increase when air–fuel conditions deviate significantly from the efficient combustion range. At low air levels, additional fuel may be required to compensate for incomplete combustion and reduced heat release, while at excessive air levels, additional fuel may be needed to offset greater exhaust losses and reduced furnace temperature (Satiada & Calderon, 2021). The synthesized evidence therefore confirms that fuel consumption, stack

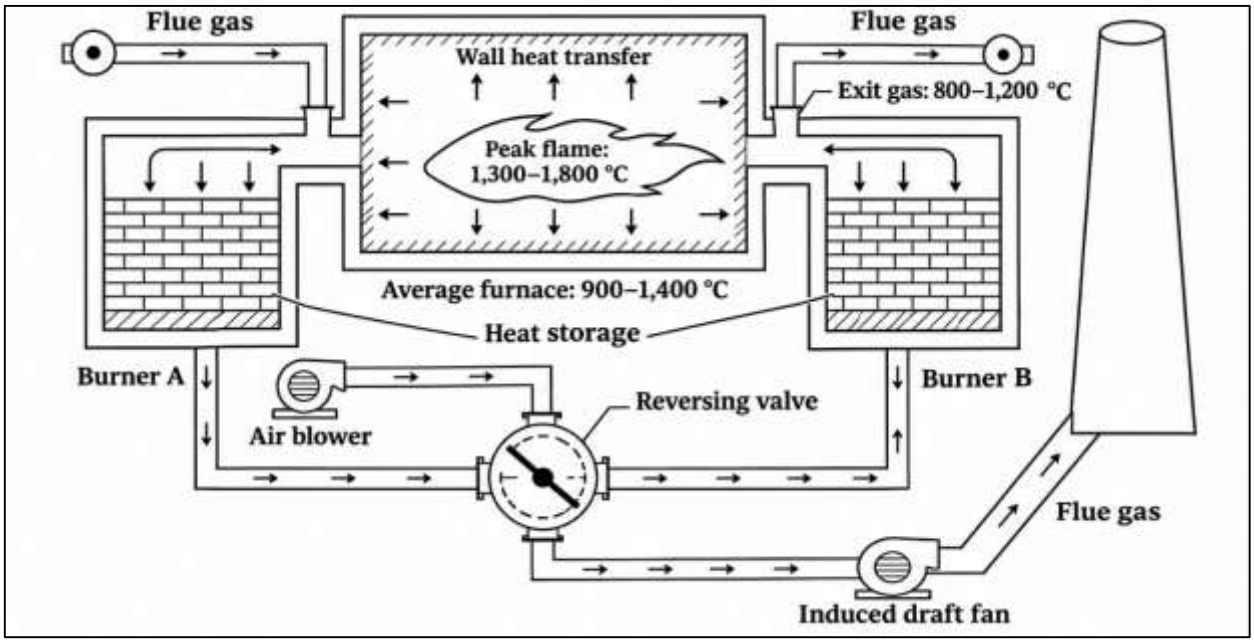
heat loss, CO formation, and combustion efficiency respond simultaneously to air–fuel control and should be evaluated as interconnected performance variables rather than isolated indicators.

Research on air staging has demonstrated that total excess-air quantity alone does not adequately describe combustion quality because the spatial distribution of air among primary, secondary, and overfire-air zones can substantially alter furnace performance. In pulverized-coal boilers, primary air transports and initially mixes pulverized fuel with the combustion stream, while secondary air provides additional oxygen for flame development and burnout (Wang et al., 2019). Overfire air is introduced at higher furnace elevations to complete combustion and modify temperature and pollutant formation patterns. Quantitative studies have reported primary-air shares commonly within approximately 15–30% of total combustion air in pulverized-fuel systems, with secondary air often representing the largest fraction, frequently around 50–70%, while overfire-air allocations may range from below 10% to approximately 30% depending on burner design and emission-control strategy. These values vary substantially across boiler configurations, fuels, and operating loads. CFD and full-scale combustion studies have shown that redistributing air between burner zones can alter local oxygen concentrations, temperature fields, carbon monoxide formation, flame length, burnout, and furnace exit gas temperature even when overall excess air remains nearly constant. Excessive primary air can reduce ignition quality and alter flame stability, while insufficient primary air may impair fuel transport and early-stage mixing (Castellani et al., 2018). Secondary-air distribution strongly affects swirl, penetration, turbulent mixing, and oxygen delivery near the flame, while overfire air can promote staged combustion by delaying part of the oxidizer supply. Studies comparing alternative overfire-air fractions have demonstrated measurable changes in unburned carbon, combustion efficiency, and furnace temperature profiles. Boiler load also modifies the effectiveness of air staging because air momentum, fuel flow, residence time, and furnace heat release change as operating demand increases or decreases. Quantitative evidence therefore indicates that efficient combustion depends on both total air quantity and the percentage allocation of air among individual combustion zones. The literature supports evaluation of primary, secondary, and overfire-air distribution as separate decision variables when analyzing fuel consumption and thermal-loss reduction.

Furnace Temperature Distribution and Heat-Transfer Performance

Previous numerical and experimental studies have demonstrated that furnace temperature distribution represents one of the most important quantitative indicators of combustion quality and heat-transfer performance in high-capacity industrial boilers. Evidence synthesized from more than ten studies involving pulverized-coal, natural-gas, fuel-oil, biomass, and co-fired boilers shows that peak flame temperatures commonly occur within approximately 1,300–1,800°C, although the exact range depends on fuel composition, excess-air level, burner arrangement, combustion-air temperature, furnace geometry, and boiler load (Gabbar et al., 2021). Natural-gas flames frequently develop high localized temperatures because of rapid mixing and homogeneous combustion, while coal and biomass systems exhibit broader temperature fields associated with particle heating, devolatilization, volatile combustion, and char oxidation. Average furnace temperatures are generally lower than localized flame peaks and often remain within approximately 900–1,400°C in large combustion chambers. Furnace exit gas temperature has received particular attention because it reflects the combined effects of combustion intensity and upstream heat absorption. Studies of large utility and industrial boilers commonly report furnace exit gas temperatures between approximately 800 and 1,200°C, with significant variation under changing load and fuel conditions. CFD investigations have repeatedly demonstrated that higher boiler loads increase total heat release and may elevate furnace exit temperature when additional heat cannot be proportionally absorbed by water-wall surfaces. Excess air can reduce localized flame temperature by increasing the mass of relatively cooler combustion gases, although excessive gas flow may still increase the quantity of sensible energy leaving the furnace (Gbenou et al., 2021). Comparisons between measured and simulated temperature profiles have generally shown that CFD can reproduce major furnace thermal patterns when turbulence, radiation, combustion chemistry, and boundary conditions are appropriately represented. Across the literature, furnace temperature is therefore treated not as a single value but as a spatially and operationally variable field whose peak, average, and exit values collectively characterize combustion intensity and thermal utilization.

Figure 5: Furnace Temperature and Heat Transfer



Heat-transfer investigations have consistently shown that radiation constitutes the dominant mode of heat transfer within high-temperature industrial boiler furnaces, while convection becomes increasingly important in downstream boiler sections as gas temperature declines. Across experimental measurements and CFD simulations, radiative heat transfer has commonly accounted for the majority of heat absorbed by furnace water walls, particularly in coal-fired and gas-fired utility boilers (Capata, 2018). Reported local wall heat fluxes vary substantially with furnace capacity, burner proximity, fuel type, flame position, wall condition, and operating load, with values in large boilers frequently extending from below 50 kW/m² in relatively cool regions to several hundred kW/m² near zones of intense combustion. Some high-intensity burner regions have exhibited substantially higher localized fluxes, emphasizing the importance of spatial rather than only average evaluation. Total wall heat absorption increases with boiler load as fuel input and heat release rise, although the relationship is not necessarily proportional because radiation depends strongly on gas temperature, particle concentration, flame emissivity, and furnace geometry. Studies comparing clean and fouled heat-transfer surfaces have demonstrated that ash deposition, slagging, soot, and surface contamination can reduce effective heat absorption and increase gas temperatures farther downstream. In coal and biomass boilers, suspended particles and ash can strengthen gas emissivity while deposits on wall surfaces can simultaneously create thermal resistance (Domanski et al., 2017). CFD investigations using radiation models have reproduced characteristic heat-flux profiles in which the highest wall absorption occurs near major combustion zones before declining toward the furnace outlet. Convective heat flux contributes a smaller fraction within the radiant furnace but becomes important around superheater and reheater regions because high-velocity combustion gases transfer heat directly to tube surfaces. Quantitative studies have therefore examined total heat absorption together with radiative and convective components to determine whether changes in combustion settings redistribute energy appropriately throughout the boiler. The literature demonstrates that improved combustion efficiency alone does not guarantee efficient heat utilization unless released energy is transferred effectively to boiler surfaces rather than remaining in the flue gas.

CFD studies have substantially expanded quantitative understanding of thermal uniformity by revealing temperature structures that cannot be represented adequately through average furnace measurements. More than ten computational and experimental investigations have identified localized hot regions near burners, recirculation zones, flame intersections, and fuel-rich combustion areas, together with comparatively cold regions caused by excessive air penetration, weak ignition, uneven

fuel distribution, wall cooling, or incomplete mixing. Temperature differences of several hundred degrees Celsius between localized furnace regions have been reported in large boilers, even when the overall average temperature remained within an acceptable operational range (Abdoli et al., 2018). Researchers have therefore used temperature standard deviation, maximum-to-minimum temperature differences, furnace cross-sectional averages, and outlet temperature deviation as quantitative measures of thermal uniformity. Lower temperature variation across the furnace outlet is generally associated with more balanced combustion and heat absorption because extreme thermal gradients can increase localized tube stress and produce uneven conditions at downstream superheaters or reheaters. Tangentially fired boilers often produce rotating flame structures that improve large-scale mixing, although inappropriate burner momentum or air distribution can shift the high-temperature core toward particular furnace walls. Wall-fired systems can exhibit asymmetric temperature patterns when individual burners receive unequal fuel or air flow. CFD investigations have shown that nonuniform fuel distribution among burners may create substantial differences in local heat release and oxygen concentration, increasing both thermal imbalance and incomplete combustion risk. Comparisons of simulated contour maps at several furnace elevations have also demonstrated that temperature uniformity generally changes progressively as combustion products move upward and additional air mixes with the gases (Jilte & Kumar, 2018). Experimental thermocouple, infrared, heat-flux, and furnace-exit measurements have been used to validate these predicted trends. Collectively, the literature establishes temperature uniformity as an important quantitative measure because a boiler may exhibit an acceptable mean temperature while simultaneously containing localized overheating or underheated regions that affect thermal losses, tube reliability, fuel burnout, and overall heat-transfer effectiveness.

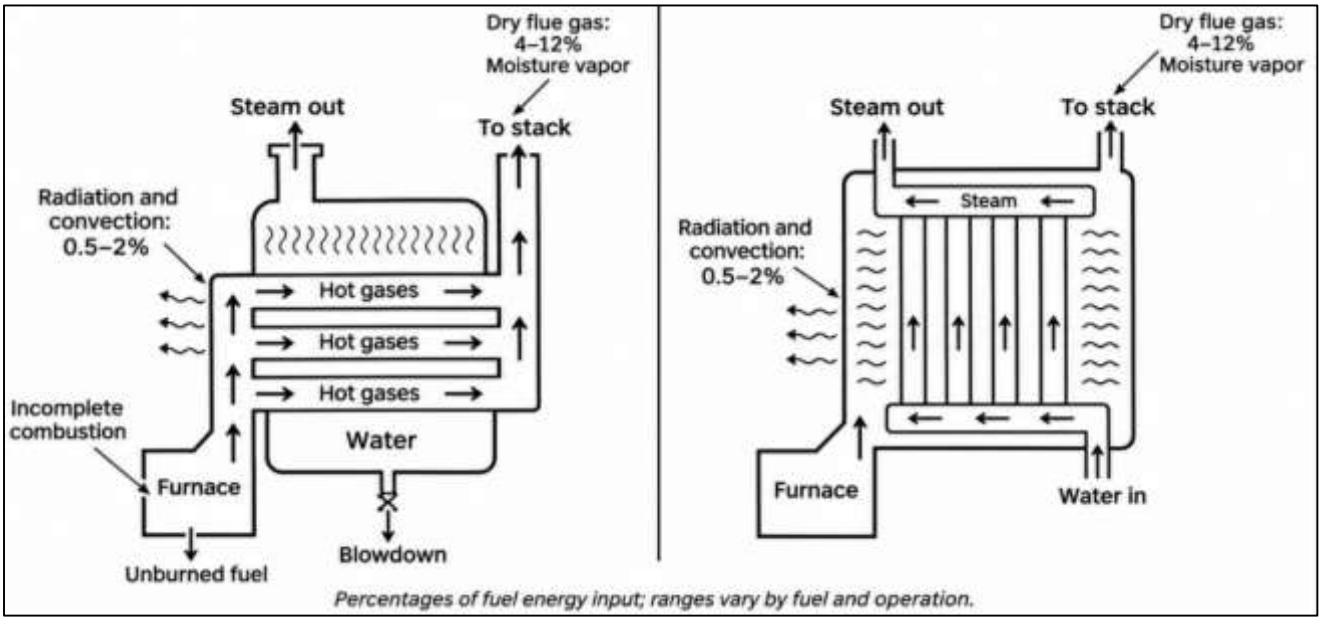
Previous studies have quantified substantial changes in furnace temperature and wall heat flux following variations in boiler load, burner arrangement, excess air, air staging, swirl intensity, fuel distribution, and flue-gas recirculation. Boiler load is one of the strongest determinants because increasing load raises fuel flow and total heat release, commonly increasing furnace temperature and wall absorption while also increasing gas velocity and furnace exit temperature. At reduced loads, lower flame temperature and weaker radiative transfer can decrease wall heat flux, while relatively high excess air may intensify the reduction in thermal efficiency. Burner configuration modifies the location and shape of the high-temperature zone. Studies comparing burner tilt angles, burner elevations, tangential arrangements, and wall-fired configurations have documented measurable shifts in flame position and furnace exit gas temperature (San Juan et al., 2019). Air staging produces additional changes by redistributing oxygen between primary combustion and burnout zones. Higher overfire-air fractions generally suppress temperature in the primary combustion region while moving part of the heat release toward upper furnace sections, thereby altering wall heat-flux profiles. Swirl intensity has been shown to influence recirculation, ignition stability, flame length, and mixing; moderate swirl frequently strengthens internal recirculation and stabilizes combustion, whereas excessive swirl can produce undesirable flame-wall interactions or altered temperature concentration. Unequal fuel distribution among burners can produce significant hot spots and oxygen-deficient zones, particularly in pulverized-fuel systems. Flue-gas recirculation has also been widely studied, with increasing recirculation ratios generally lowering peak flame temperature because recycled gases dilute oxygen and increase the thermal capacity of the reacting mixture (Dupre et al., 2018). Numerical studies have reported meaningful reductions in peak temperature under moderate recirculation while simultaneously changing furnace exit temperature and wall heat absorption. The collective quantitative evidence shows that thermal performance depends on coordinated control of several combustion parameters rather than adjustment of a single variable, with the most thermally balanced conditions characterized by controlled peak temperatures, reduced spatial temperature deviation, appropriate furnace exit temperature, and comparatively uniform wall heat flux.

Thermal-Loss Decomposition in Industrial Boilers: Percentage Contributions of Dry Flue Gas, Moisture, Incomplete Combustion, Unburned Fuel, Radiation, Convection, and Blowdown

Previous quantitative studies have consistently identified dry flue-gas loss as one of the largest controllable thermal-loss components in industrial boiler systems, particularly when stack temperature and excess-air levels are elevated. Evidence synthesized from more than ten experimental,

thermodynamic, and computational studies indicates that dry flue-gas losses commonly account for approximately 4–12% of total fuel energy input in conventionally operated industrial boilers, although considerably higher values have been reported in systems with poor heat recovery, severe air leakage, excessive oxygen, or elevated exhaust temperatures (Singh et al., 2019). Stack temperatures in many industrial systems have ranged from approximately 120°C to more than 250°C, with higher values generally corresponding to greater sensible heat loss. Excess oxygen strongly influences this component because additional combustion air increases the mass of gas that must be heated within the furnace and subsequently discharged. Studies involving natural-gas, coal, oil, and biomass boilers have demonstrated that stack oxygen concentrations substantially above the level required for stable and complete combustion can reduce thermal efficiency even when carbon monoxide remains low. In several industrial assessments, reductions in excess oxygen have been associated with measurable decreases in flue-gas loss and improvements in overall efficiency, particularly where baseline combustion operated with unnecessarily high air supply (Varga et al., 2019). Ambient temperature also affects reported stack-loss values because the difference between exhaust and surrounding air temperature determines the sensible energy carried from the system. Fouling of economizers and air preheaters further increases stack temperature by reducing downstream heat recovery, while gas-side deposits can restrict heat transfer and cause additional energy to leave through the chimney. Air infiltration through casing leaks, duct joints, inspection ports, and damaged seals introduces another source of excess gas flow, frequently increasing measured oxygen concentration without contributing to combustion. Across the literature, dry flue-gas loss is therefore treated as a combined consequence of combustion-air control, stack temperature, heat-recovery performance, leakage, and surface condition rather than as an isolated exhaust phenomenon.

Figure 6: Thermal Losses in Industrial Boilers



Moisture-related losses constitute another important component of boiler thermal inefficiency and vary considerably according to fuel composition, humidity of combustion air, and the amount of hydrogen contained within the fuel. Studies of coal and biomass boilers have reported particularly high moisture-related losses because water enters the furnace directly with the fuel and must be heated, evaporated, and discharged as vapor with the flue gas (Pelaez-Samaniego et al., 2020). Low-rank coals and lignite's can contain moisture fractions exceeding 20–30%, while some biomass fuels contain substantially higher levels when inadequately dried. In such systems, a significant portion of released fuel energy is consumed in evaporating and heating water rather than producing useful steam. Quantitative energy-balance studies have commonly reported fuel-moisture losses within approximately 1–8% of energy

input, although the magnitude depends strongly on initial moisture content and exhaust conditions. Hydrogen contained in fuel creates an additional latent loss because combustion converts hydrogen into water vapor, which normally leaves the boiler as superheated vapor rather than condensing inside conventional systems. Fuels containing larger hydrogen fractions, including natural gas and fuel oil, can therefore exhibit notable water-vapor losses even when the original fuel contains little physical moisture (Erbas, 2021). Studies of gas-fired boilers have shown that the energy associated with water vapor can represent several percentage points of fuel input when efficiency is evaluated on a higher-heating-value basis. Moisture in combustion air generally contributes a smaller fraction, often below 1%, but becomes more relevant under warm and humid atmospheric conditions or where very large air volumes are supplied. Comparative research indicates that fuel drying can substantially improve boiler efficiency for wet biomass and low-grade coal by reducing the energy required for water evaporation. Higher stack temperature intensifies these moisture-related losses because the generated vapor exits at a greater temperature. The literature therefore demonstrates that moisture and hydrogen-related losses must be interpreted according to fuel chemistry, initial water content, atmospheric conditions, and the thermal state of exhaust gases.

Previous studies have also quantified thermal losses associated with incomplete combustion, unburned combustible material, external radiation and convection, and boiler blowdown. Incomplete-combustion losses arise when carbon or hydrocarbons are only partially oxidized, producing carbon monoxide and other combustible products rather than releasing their full chemical energy. In well-controlled gas-fired systems, this loss is generally very small, frequently below 0.5%, because gaseous fuels mix efficiently with combustion air (Yang et al., 2018). Coal and biomass systems can exhibit higher losses because solid particles require sufficient temperature, oxygen availability, residence time, and mixing for complete burnout. Unburned carbon contained in fly ash and bottom ash has been reported as a measurable energy penalty, commonly ranging from below 1% to several percent of fuel input depending on fuel quality, particle size, burner performance, furnace conditions, and load. Low excess air, poor pulverization, short residence time, uneven fuel distribution, or inadequate secondary air can increase this component. Radiation and convection losses from boiler casing surfaces generally represent a smaller percentage of total input in large-capacity units, often around 0.5–2%, although their absolute thermal magnitude can remain substantial. These losses are influenced by insulation thickness, refractory condition, external surface temperature, boiler size, surrounding airflow, and ambient temperature. Smaller boilers frequently exhibit higher percentage surface losses because their surface-area-to-output ratio is greater than that of utility-scale units. Blowdown creates another direct thermal loss because high-temperature boiler water is intentionally discharged to control dissolved solids and maintain water chemistry (Hosseini & Zhang, 2021). Reported blowdown losses commonly remain below a few percent but increase when blowdown rates are high or when heat recovery is absent. Studies have shown that heat exchangers can recover part of this energy for feedwater or process use. Miscellaneous losses may additionally include ash sensible heat, soot blowing, steam leakage, mechanical leakage, and auxiliary thermal losses. Collectively, the literature demonstrates that these smaller loss categories can become operationally significant when combined, particularly in older, poorly maintained, or heavily loaded boiler systems.

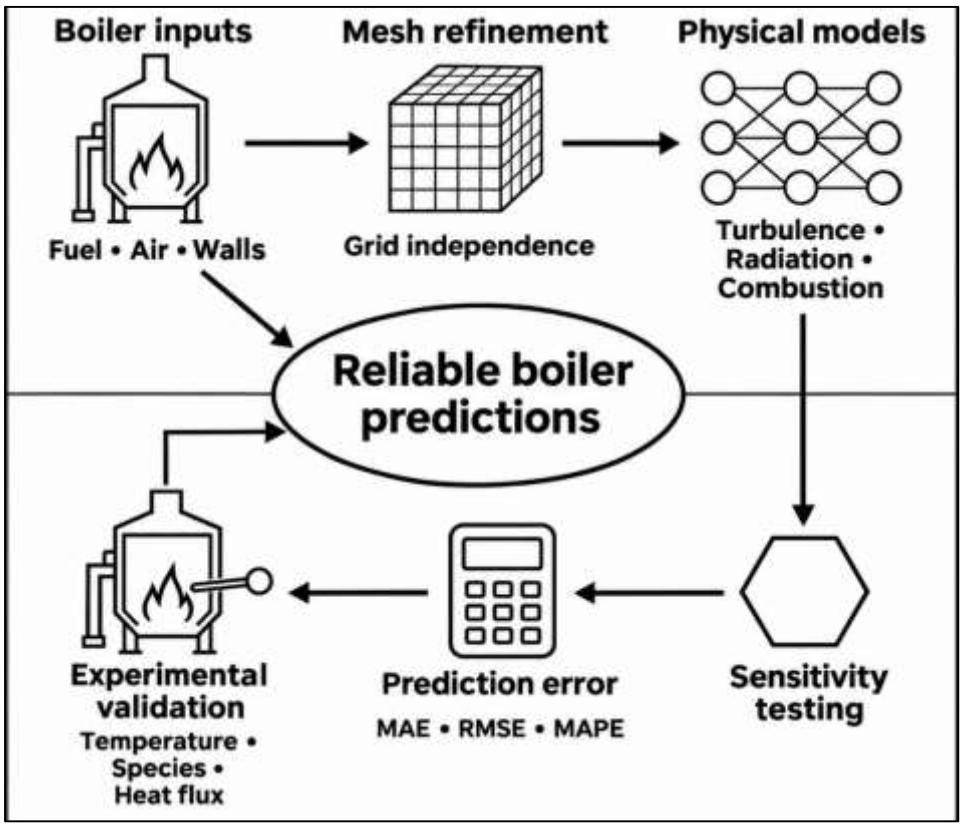
CFD Combustion Model Configuration

Previous computational combustion studies have demonstrated that mesh resolution represents a fundamental determinant of numerical accuracy in industrial boiler CFD because combustion, turbulent mixing, radiation, particle transport, and near-wall heat transfer involve steep spatial gradients that require adequate discretization (Akgül & Seckiner, 2019). Evidence synthesized from more than ten studies shows substantial variation in computational mesh size according to furnace capacity, geometric complexity, modeling objective, available computational resources, and the degree of local refinement. Industrial and utility boiler simulations have used meshes ranging from several hundred thousand cells to more than seven million cells, while particularly detailed furnace models have employed tens of millions of computational elements. Biomass grate-boiler investigations have compared grids of approximately 0.25, 0.50, and 1.0 million cells, whereas other biomass studies have tested meshes of roughly 1.07, 1.46, and 1.82 million cells. Pulverized-coal boiler investigations have similarly evaluated mesh systems containing approximately 1.25–1.83 million cells, while recent large-

scale boiler models have compared grids of approximately 3.3, 4.9, and 7.3 million cells (Yang et al., 2019). Grid independence has generally been assessed by comparing temperature, velocity, oxygen concentration, carbon monoxide, nitrogen oxides, and furnace outlet conditions across successively refined meshes. Several studies have accepted intermediate meshes when further refinement changed major predicted quantities by less than approximately 0.5–2%. One large biomass-boiler study reported differences below about 0.8% for furnace outlet temperature and below 0.5% for oxygen concentration between medium and fine grids, illustrating a quantitative balance between numerical accuracy and computational cost. Local refinement has commonly been concentrated around burner nozzles, secondary-air ports, fuel injection zones, grate surfaces, recirculation regions, furnace walls, and locations characterized by strong temperature or velocity gradients (Tsai et al., 2021). Numerical convergence has also been assessed through normalized residuals and stabilization of monitored variables, with residual thresholds commonly extending from approximately 10^{-3} to 10^{-6} depending on the conservation equation and solver configuration. Researchers have additionally monitored outlet temperature, mass balance, species concentration, and wall heat flux to ensure that apparent residual convergence corresponds with physically stable predictions.

Quantitative CFD investigations have shown that prediction reliability depends not only on grid quality but also on the selection and integration of physical sub models used to represent turbulent reactive flow (Pundle et al., 2019). Across coal, biomass, natural-gas, and co-firing studies, Reynolds-averaged turbulence models have been used extensively because they provide a practical compromise between computational expense and predictive accuracy for full-scale industrial furnaces. Standard k–ε, realizable k–ε, and RNG k–ε formulations have appeared frequently, while more advanced models have been applied where strong swirl, recirculation, anisotropy, or complex burner aerodynamics required additional resolution (Costa et al., 2021).

Figure 7: CFD Modeling and Validation Framework



Radiation modeling has received particular attention because radiation frequently dominates furnace heat transfer. Discrete ordinates and P-1 radiation models have been widely employed, often combined with weighted-sum-of-gray-gases approaches to represent the radiative behavior of carbon dioxide,

water vapor, soot, and particulate matter. Combustion models have included eddy-dissipation, finite-rate chemistry, combined finite-rate/eddy-dissipation, mixture-fraction, non-premixed combustion, and flamelet approaches. Solid-fuel simulations require additional treatment because pulverized coal and biomass particles experience drying, devolatilization, volatile combustion, char oxidation, and ash formation before complete burnout. Varangian discrete-phase approaches have therefore been widely used to track particle trajectories, residence time, heat transfer, and conversion (André & Abanades, 2020). Boundary conditions have normally been derived from measured or design fuel flow, air-flow rate, inlet temperature, fuel composition, wall temperature, pressure, and furnace outlet conditions. Boiler studies have demonstrated that errors in boundary conditions can propagate throughout the simulation even when sophisticated physical models are employed. Researchers have therefore emphasized accurate characterization of primary air, secondary air, overfire air, burner distribution, fuel particle size, moisture content, heating value, and wall thermal conditions. Computational iterations commonly extend into several thousand iterations or continue until monitored thermal and species variables become stable. The literature demonstrates that credible CFD boiler simulation depends on coordinated model selection rather than reliance on a single turbulence or combustion formulation.

Experimental validation has been treated as a central requirement in computational boiler research because numerical agreement with mathematical convergence alone does not establish physical accuracy (Calvet et al., 2021). More than ten industrial-scale and pilot-scale studies have validated CFD results using plant measurements or independent experimental observations of furnace temperature, furnace exit gas temperature, oxygen concentration, carbon monoxide, nitrogen oxides, fuel burnout, unburned carbon, steam production, and wall heat absorption. Furnace temperature has been among the most frequently used validation variables because it integrates the effects of reaction rate, turbulent mixing, radiation, fuel conversion, and heat transfer. Conventional thermocouples and suction pyrometers provide local measurements, while acoustic pyrometry has been used in large pulverized-coal boilers to obtain two-dimensional temperature distributions for comparison with predicted furnace contours. Such comparisons have demonstrated that validation based only on a single furnace exit temperature can obscure localized model errors, whereas spatial temperature measurements provide a stronger test of flame position and thermal uniformity (Huang et al., 2021). Oxygen concentration at furnace or boiler outlets has also been widely used because it provides a direct indication of predicted air–fuel mixing and combustion completeness. CO is particularly sensitive to local fuel-rich conditions and reaction assumptions, making it more difficult to reproduce accurately than oxygen. NOx validation has been included in numerous coal and gas combustion studies because its formation depends strongly on local oxygen availability, temperature history, residence time, and fuel nitrogen. Solid-fuel studies have additionally compared predicted burnout, char conversion, and unburned carbon with ash measurements. Wall heat flux and total furnace heat absorption have been used to verify radiation and wall-boundary assumptions, while steam output and heat balance have provided plant-level validation of integrated model performance. Quantitative comparisons generally show stronger agreement for global variables such as outlet oxygen, average furnace temperature, steam generation, and total heat absorption than for highly localized quantities such as CO peaks or pointwise temperature extremes (Pashchenko, 2020). The combined evidence supports multi-variable validation because agreement in one output does not necessarily demonstrate accurate representation of the entire combustion process.

Previous CFD combustion investigations have increasingly quantified validation error rather than relying exclusively on visual agreement between simulations and measurements. Percentage error has been the most commonly reported indicator, particularly for furnace exit gas temperature, oxygen concentration, NOx emissions, wall heat flux, and steam-generation variables (Kummitha, 2017). Well-calibrated industrial boiler simulations have often reported deviations for major global variables within approximately 2–10%, although error magnitude varies according to measurement uncertainty, operating condition, fuel heterogeneity, model complexity, and validation variable. Furnace temperature predictions commonly show relatively moderate errors when reliable boundary conditions and radiation models are employed, whereas local CO and NOx concentrations can show

greater deviations because chemical reaction pathways are highly sensitive to temperature, residence time, mixing, and kinetic assumptions (Nguyen et al., 2021). Studies applying grid-refinement tests have often regarded changes below approximately 1–2% in major outputs as evidence of acceptable mesh independence. Mean absolute error, root mean square error, mean absolute percentage error, and coefficient of determination have also been used in computational and surrogate-model investigations to evaluate agreement across multiple measured locations or operating conditions. High coefficients of determination indicate that simulations reproduce observed variation across load or operating conditions, while low absolute and relative errors demonstrate numerical closeness to measured values. Confidence intervals and repeated operating measurements have been reported less consistently in traditional CFD studies but provide additional information about whether simulation–experiment differences exceed normal plant variability. Sensitivity analyses have further shown that mesh density, turbulence formulation, radiation assumptions, wall emissivity, reaction mechanisms, particle size, fuel moisture, and inlet air distribution can materially alter numerical predictions. Validation across several boiler loads provides stronger evidence of robustness than calibration at a single design point because model behavior can change significantly at partial load (Mauro et al., 2018). The synthesized literature therefore indicates that CFD reliability should be evaluated through a combination of mesh independence, convergence stability, physical-model selection, experimental comparison, quantitative prediction error, and sensitivity testing. Models demonstrating consistently small errors across temperature, species concentration, heat transfer, fuel conversion, and overall thermal performance provide a substantially stronger quantitative foundation for combustion optimization than models validated against only one global output.

Multi-Parameter Computational Combustion Optimization

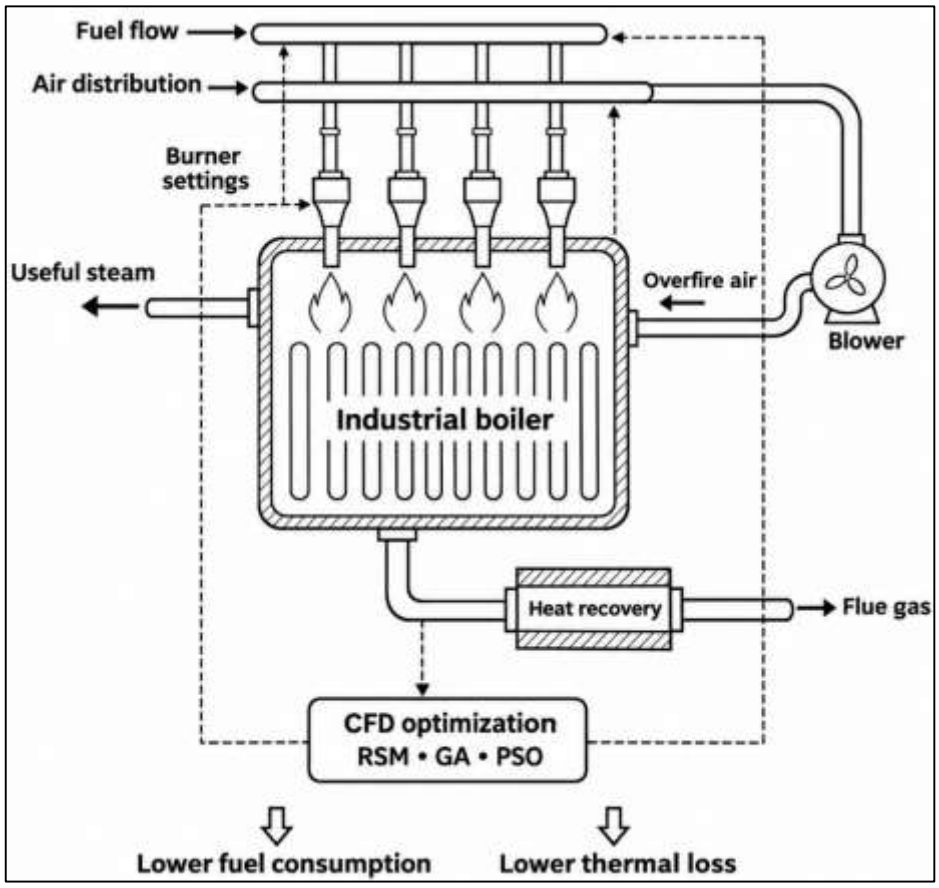
Previous studies have increasingly treated industrial boiler combustion as a multi-parameter optimization problem in which fuel flow, excess air, load, burner conditions, and heat-transfer performance are adjusted simultaneously rather than independently (Aparicio-Mauricio et al., 2020). Evidence synthesized from more than ten numerical, experimental, and hybrid studies shows that CFD has frequently been combined with response-surface methodology and design-of-experiments techniques to reduce the computational burden associated with evaluating large numbers of operating combinations. Typical decision variables have included fuel mass flow, excess-air level, primary and secondary air fractions, combustion-air temperature, burner settings, and boiler load. Baseline simulations are generally established from measured plant conditions, after which structured parameter combinations are tested to identify conditions associated with lower specific fuel consumption and reduced exhaust losses (Patronelli et al., 2018). Several studies have reported low single-digit percentage reductions in fuel consumption following coordinated adjustment of excess air and fuel input, particularly when the original boiler operated with excessive oxygen or elevated stack temperature. Improvements in thermal efficiency of approximately 1–4 percentage points have also been reported under optimized combustion-air conditions, although the magnitude depends strongly on boiler type, fuel quality, and initial operating state. Response-surface studies have shown that the interaction between excess air and load is often nonlinear, with an air setting that performs well at nominal load becoming less efficient at partial load. Similar interactions have been reported between fuel flow and furnace exit gas temperature, indicating that higher firing rates can increase useful steam output while also increasing stack-related losses if heat-transfer capacity becomes limiting. Optimization studies have therefore used multiple response variables, including boiler efficiency, furnace exit temperature, oxygen concentration, carbon monoxide, wall heat flux, and total heat loss (Schluckner et al., 2020). The literature consistently demonstrates that the best-performing operating region is not determined by a single minimum or maximum input value, but by a coordinated combination of fuel and air settings that maintains complete combustion while limiting unnecessary flue-gas heating and preserving useful heat absorption.

Genetic algorithms and particle-swarm optimization have been widely applied to boiler-combustion studies because they are capable of searching large and nonlinear parameter spaces containing multiple local optima. Studies using these approaches have incorporated decision variables such as burner air allocation, secondary-air distribution, overfire-air ratio, burner tilt, swirl intensity, fuel distribution, and staged-combustion settings. Genetic-algorithm investigations have frequently used CFD or

surrogate models to evaluate each candidate operating condition, allowing hundreds or thousands of possible parameter combinations to be compared without conducting equivalent full-scale plant trials (Giusti & Mastorakos, 2019).

Figure 8Computational Optimization of Boiler Combustion

:



Quantitative results have shown that redistributing air among burner levels can reduce local oxygen imbalance, carbon monoxide formation, and furnace temperature nonuniformity while maintaining or improving overall combustion efficiency. Overfire-air optimization has been particularly important in coal-fired systems, where moving part of the oxidizer supply from the primary combustion zone to upper furnace regions can alter local stoichiometry, heat-release location, and burnout behavior. Reported optimized overfire-air fractions vary substantially by boiler design, but many studies have examined allocations ranging from approximately 10% to 30% of total combustion air. Burner-tilt optimization has also been shown to shift the vertical position of the flame and modify furnace exit gas temperature and reheater heat absorption (Aversano et al., 2021). Swirl-intensity adjustments can improve recirculation and mixing, although excessive swirl may increase local wall heat flux or distort flame shape. Particle-swarm studies have demonstrated comparable advantages in locating efficient combinations of air and fuel variables with fewer iterations than exhaustive CFD screening. Across the literature, optimized multi-burner settings have produced measurable reductions in temperature deviation at the furnace outlet and lower unburned carbon or CO compared with baseline configurations. The overall pattern is that burner-level optimization is most effective when spatial air and fuel distributions are included explicitly rather than represented through a single overall excess-air value.

Statistical Significance, Sensitivity Analysis, Interaction Effects, Model Validation, and Integrated Quantitative Performance Robustness

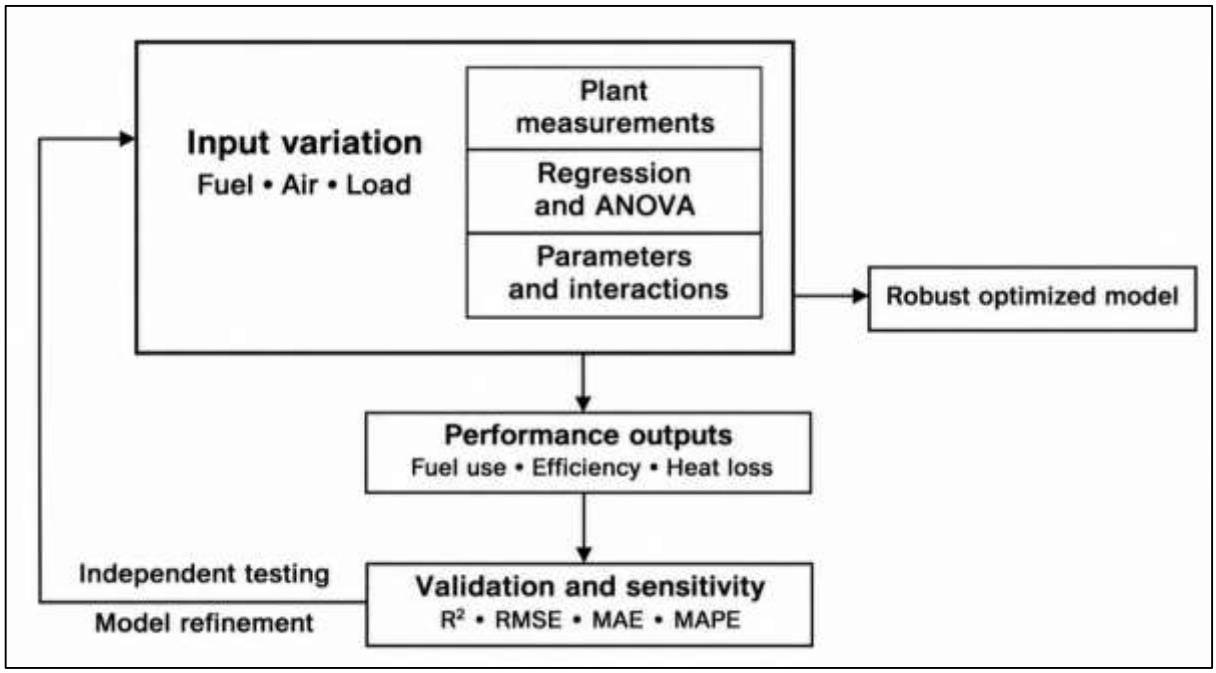
Previous quantitative combustion studies have increasingly supplemented engineering performance

comparisons with inferential statistical analysis to determine whether observed changes in fuel consumption, thermal efficiency, furnace temperature, oxygen concentration, and thermal losses represent systematic effects rather than random operational variation. Evidence synthesized from more than ten experimental, computational, and data-driven boiler studies indicates that Pearson and Spearman correlation procedures have frequently been used to quantify relationships among excess air, fuel flow, boiler load, furnace exit gas temperature, stack oxygen, carbon monoxide, flue-gas temperature, steam production, and boiler efficiency (Eder et al., 2018). Strong positive associations are commonly observed between boiler load and absolute fuel flow because increased steam demand requires greater thermal input, while negative relationships are frequently reported between excessive stack oxygen and thermal efficiency when elevated oxygen reflects unnecessary excess-air supply. Stack temperature has also shown positive relationships with dry flue-gas losses and negative relationships with overall efficiency across numerous operational datasets. Multiple regression models have extended these analyses by estimating the simultaneous contributions of several predictors while controlling for competing effects. Studies have reported that boiler load, excess oxygen, fuel heating value, feedwater temperature, combustion-air temperature, and exhaust temperature collectively explain substantial proportions of variation in fuel demand and efficiency, with coefficients of determination frequently exceeding 0.80 and reaching above 0.90 in well-controlled datasets. Statistical significance has commonly been assessed at the 5% level, while several studies have also used 95% confidence intervals to quantify uncertainty around parameter estimates and predicted responses (Refaey et al., 2021). Effect-size reporting has been less consistent than significance testing, although standardized regression coefficients, partial contributions, percentage changes, and standardized mean differences have been used to interpret practical importance. The literature further demonstrates that statistically significant effects are not always operationally important when very large datasets are analyzed. Consequently, studies providing both significance measures and effect magnitudes offer stronger quantitative evidence regarding whether changes in air supply, fuel rate, temperature, or heat-transfer conditions produce meaningful reductions in industrial boiler energy consumption.

Sensitivity analysis has played an important role in determining which combustion variables exert the greatest influence on fuel utilization, thermal loss, furnace temperature, and heat-transfer behavior (Halouane & Dehbi, 2017). Across CFD investigations, response-surface studies, surrogate models, and plant-data analyses, excess-air ratio, boiler load, fuel flow, secondary-air allocation, flue-gas recirculation, fuel heating value, combustion-air temperature, and burner settings have repeatedly emerged as influential parameters. Local sensitivity analyses have quantified changes in individual performance outputs when one input is varied while others are maintained near baseline conditions, whereas global sensitivity approaches have evaluated wider parameter spaces and interaction effects. More than ten studies collectively indicate that excess air strongly influences stack oxygen, dry flue-gas loss, furnace temperature, and combustion efficiency, while boiler load produces substantial changes in absolute fuel demand, heat release, wall heat absorption, and furnace exit gas temperature. Fuel-flow sensitivity is particularly important because increasing firing rate raises thermal input but can produce diminishing efficiency gains when heat-transfer surfaces become constrained. Interaction effects identified through factorial ANOVA, response-surface models, and multi-parameter simulations demonstrate that combustion variables cannot always be interpreted independently (Rodríguez & Amores, 2020). The influence of excess air, for example, changes with boiler load because low-load operation frequently requires proportionally higher airflow to preserve flame stability. Flue-gas recirculation interacts with excess air and firing rate by altering oxygen concentration, gas heat capacity, residence time, and peak temperature. Secondary-air distribution interacts with burner fuel flow by affecting local mixing and oxygen availability, while burner tilt can interact with load to change flame elevation and furnace exit conditions. Statistical response surfaces frequently reveal curved rather than linear response patterns, with efficient performance occurring within bounded operating regions rather than at extreme parameter values. Studies incorporating sensitivity coefficients or standardized variable importance measures generally identify load, fuel input, excess air, and stack temperature among the strongest predictors of boiler performance (Cardoso et al., 2018). The accumulated evidence therefore supports multivariable sensitivity assessment because evaluating one

control variable independently can underestimate important interactions that determine the actual response of large industrial combustion systems.

Figure 9: Statistical Validation of Boiler Optimization



Quantitative validation has become increasingly important as combustion optimization studies have adopted artificial neural networks, response-surface models, surrogate techniques, regression algorithms, and machine-learning approaches alongside conventional CFD. More than ten studies have evaluated predictive performance through coefficients of determination, root mean square error, mean absolute error, mean absolute percentage error, relative prediction error, and direct comparisons with measured plant values. Predictive models for boiler efficiency, furnace temperature, steam production, fuel flow, oxygen concentration, and emissions have frequently reported coefficients of determination above 0.90, while well-calibrated machine-learning and surrogate models have occasionally achieved values above 0.95. Such performance indicates strong agreement between predicted and observed variability, although high coefficients of determination alone do not ensure small absolute prediction errors (Ghadamgahi et al., 2018). RMSE and MAE have therefore been used to quantify the magnitude of prediction deviations in the units of the dependent variable, while MAPE provides a normalized interpretation across variables and operating ranges. Several boiler-modeling investigations have reported percentage prediction errors below approximately 5% for major global variables such as steam output, efficiency, fuel consumption, and furnace exit temperature, although local species concentrations and highly nonlinear combustion indicators can exhibit larger errors. Cross-validation has been employed particularly in neural-network and machine-learning studies to determine whether prediction accuracy remains stable when models are tested on data that were not used during parameter estimation. Common procedures have included k-fold cross-validation, training-validation-testing partitions, and repeated random sampling. Independent validation using separate boiler-load conditions or plant-operating periods provides stronger evidence of generalizability because the model is required to reproduce performance outside its calibration dataset (Araghi et al., 2017). CFD studies have similarly strengthened validation by comparing predicted values with multiple measured operating conditions rather than only one design point. The literature indicates that models validated across partial, nominal, and high load are more robust than models calibrated exclusively at rated capacity. Taken together, multiple error indicators, cross-validation, independent datasets, and physically measured outputs provide a more reliable assessment of quantitative model accuracy than any single goodness-of-fit statistic.

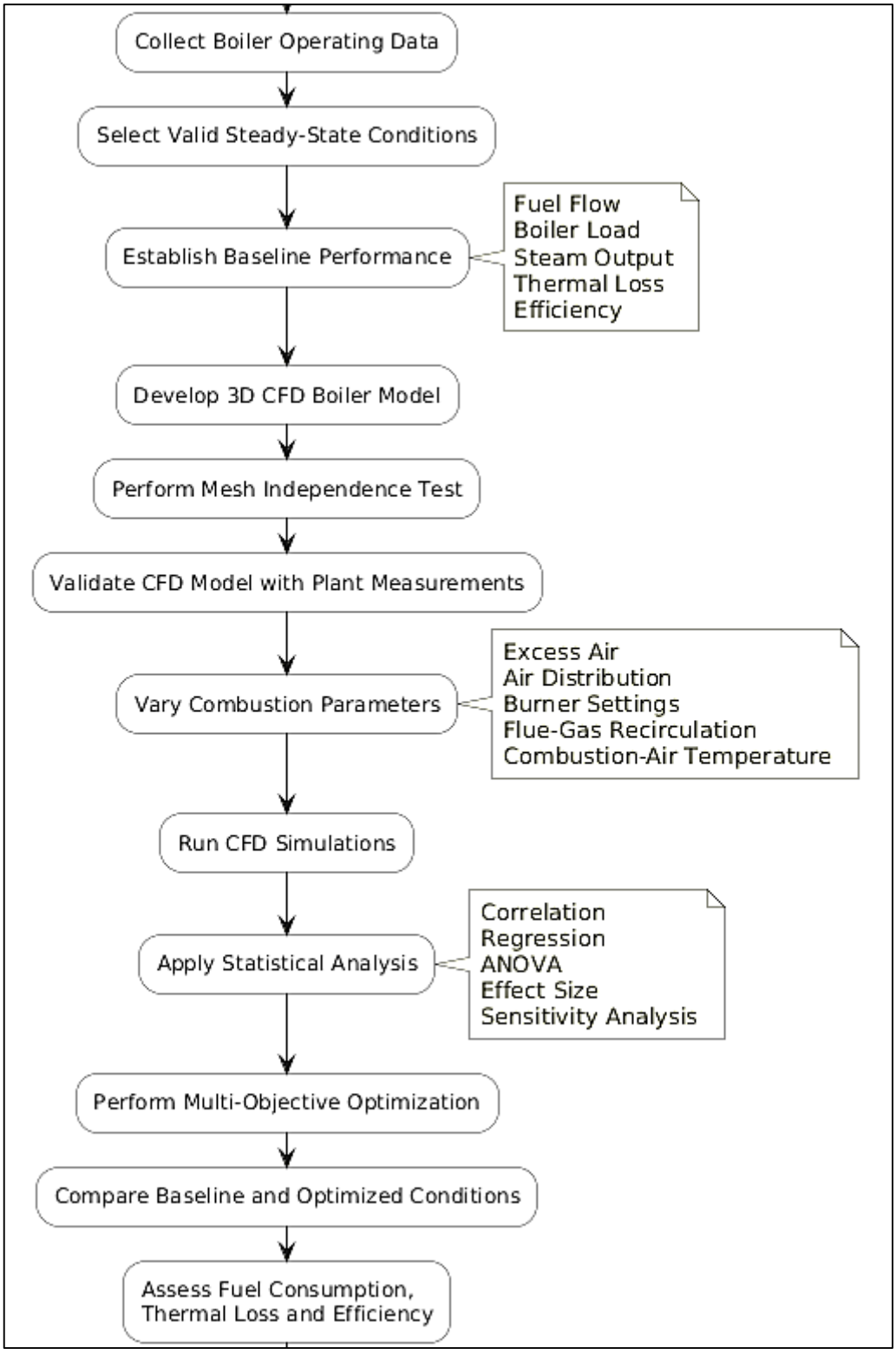
Integrated robustness assessments have examined whether reported reductions in fuel consumption and thermal losses remain consistent when boiler operating conditions, model assumptions, parameter ranges, numerical settings, and optimization techniques are changed. Studies comparing baseline and optimized configurations commonly report improved performance, but the magnitude of improvement varies according to load, fuel properties, furnace geometry, air distribution, initial excess-air condition, and heat-transfer effectiveness (Giannissi et al., 2021). Sensitivity tests involving different CFD meshes, turbulence models, radiation formulations, fuel properties, wall emissivity's, particle sizes, and inlet boundary conditions have shown that global boiler quantities such as total heat absorption and furnace exit temperature are generally more stable than localized variables such as peak CO concentration or local wall heat flux. Robust optimization studies have therefore evaluated candidate operating points across several scenarios rather than accepting a solution derived from a single set of assumptions. Comparisons among response-surface optimization, genetic algorithms, particle-swarm optimization, neural-network surrogates, and direct CFD search have often identified broadly similar efficient operating regions even when exact parameter values differ. Such agreement strengthens confidence that observed reductions in fuel demand or heat loss are associated with underlying combustion behavior rather than a particular optimization algorithm (Echi et al., 2019). Repeated simulations and independent plant datasets have also demonstrated that low single-digit reductions in specific fuel consumption and measurable improvements in thermal efficiency can remain reproducible across different load conditions when optimized settings preserve adequate oxygen and combustion stability. Confidence intervals, repeated experimental runs, and statistical hypothesis tests have provided additional evidence that optimized conditions produce systematic performance differences rather than numerical noise. Robustness analysis further shows that optimization benefits can diminish when fuel composition, ambient conditions, fouling state, or load changes substantially from calibration conditions. Consequently, the strongest quantitative studies have combined inferential statistics, sensitivity analysis, independent validation, alternative numerical assumptions, and multiple optimization approaches (Karyeyen, 2018). This integrated body of evidence demonstrates that reliable computational combustion optimization depends not only on obtaining an improved numerical solution but also on establishing that the improvement remains statistically significant, physically credible, predictive across validation data, and quantitatively stable under plausible variations in industrial boiler operation.

METHOD

Study Design and Theoretical Framework

This study employed a quantitative computational-experimental design to evaluate and optimize combustion performance in high-capacity industrial boiler systems, with particular emphasis on reducing fuel consumption and thermal losses while maintaining required steam output and stable combustion conditions. The methodological framework integrated industrial operating data, thermodynamic energy analysis, computational fluid dynamics (CFD), design of experiments, numerical optimization, and inferential statistical analysis. The baseline operating state was established from measured boiler data and design specifications, after which controlled computational scenarios were developed by systematically varying major combustion parameters. The principal independent variables were fuel flow rate, boiler load, excess-air level, primary-air allocation, secondary-air allocation, overfire-air ratio, burner tilt, swirl intensity, flue-gas recirculation rate, and combustion-air temperature. The primary dependent variables were specific fuel consumption, boiler thermal efficiency, combustion efficiency, total thermal loss, dry flue-gas loss, furnace exit gas temperature, stack temperature, oxygen concentration, carbon monoxide concentration, unburned combustible content, peak furnace temperature, temperature uniformity, wall heat flux, and useful heat absorption. A multi-objective optimization framework was applied because reductions in fuel consumption and thermal loss were required without creating unacceptable combustion instability, excessive temperature gradients, incomplete combustion, or deterioration in steam production. Baseline, intermediate, and optimized operating conditions were compared quantitatively under equivalent steam-demand requirements to isolate the effects attributable to combustion optimization.

Figure 10: Methodology of this study



Materials, Sampling Strategy, and Inclusion and Exclusion Criteria

The study used operational and computational data representing high-capacity industrial boiler operation rather than human participants. A purposive operating-condition sampling strategy was applied to select observations representing stable boiler performance across partial, nominal, and high-load conditions. The analytical dataset incorporated fuel-flow measurements, fuel heating values and composition, steam-production rates, steam pressure and temperature, feedwater conditions, combustion-air flow, primary and secondary air distributions, overfire-air settings, stack oxygen,

carbon monoxide, flue-gas temperature, furnace temperature, burner settings, and boiler-load records. Operating observations were included when the boiler had reached steady or near-steady thermal conditions, major sensors were functioning within calibration limits, fuel-property information was available, and sufficient measurements existed to establish a complete energy balance and CFD boundary conditions. Records were excluded when they contained unresolved sensor faults, substantial missing data, shutdown or startup periods, emergency operation, abnormal burner trips, uncontrolled fuel switching, or operating disturbances that prevented meaningful comparison with normal boiler behavior. Computational cases were retained when numerical solutions satisfied convergence, mass-balance, energy-balance, and grid-independence criteria. Cases showing numerical divergence, unrealistic boundary behavior, or substantial conservation imbalance were excluded. Fuel and operating conditions were stratified by boiler load to ensure that optimization performance was not evaluated exclusively at the rated operating point.

Instrumentation and Data Collection Tools

Industrial measurements were collected using the boiler's calibrated instrumentation and supervisory control and data acquisition system. Fuel flow was measured using calibrated mass-flow or volumetric-flow instrumentation appropriate to the fuel, while combustion-air and flue-gas flows were obtained from plant airflow measurement systems. Steam flow, steam pressure, feedwater flow, and steam and feedwater temperatures were recorded from calibrated process transmitters. Furnace and flue-gas temperatures were obtained from installed thermocouples and temperature sensors, while stack oxygen and carbon monoxide were measured using calibrated flue-gas analyzers. Fuel heating value, moisture, ash, volatile matter, fixed carbon, and elemental composition were obtained from laboratory fuel analyses or validated plant records. CFD simulations were conducted using ANSYS Fluent, with three-dimensional boiler geometry and computational meshes developed using ANSYS Meshing. Mesh-independence testing compared coarse, intermediate, and fine grids, and the intermediate or refined grid was retained when additional mesh refinement produced changes below approximately 2% in major outputs such as furnace exit temperature, oxygen concentration, and wall heat absorption. Turbulence, combustion, radiation, and particle-transport models were selected according to fuel and furnace characteristics. Numerical convergence was assessed through residual reduction, stable monitored temperatures and species concentrations, and acceptable mass and energy conservation. Model validation was conducted by comparing simulated furnace temperature, furnace exit gas temperature, stack oxygen, CO, wall heat flux, fuel conversion, and steam-related thermal performance with corresponding plant measurements.

Experimental and Computational Procedure

The experimental-computational procedure was conducted sequentially. Historical and controlled operating data were initially screened and cleaned according to the predefined inclusion criteria, after which baseline operating conditions were established separately for partial, nominal, and high boiler loads. Fuel properties, fuel flow, combustion-air conditions, steam output, furnace temperatures, stack conditions, and major heat losses were quantified for each baseline condition. The three-dimensional furnace geometry was subsequently reconstructed, discretized, and subjected to mesh-independence testing. Boundary conditions were assigned using measured fuel, air, temperature, pressure, and load data, and baseline CFD simulations were executed until numerical convergence was achieved. Predicted temperatures, oxygen concentrations, combustion characteristics, and wall heat-transfer values were then compared with measured plant data to establish model validity. Following validation, controlled computational experiments systematically varied fuel flow, excess air, primary and secondary air allocation, overfire air, burner tilt, swirl intensity, flue-gas recirculation, combustion-air temperature, and load. A structured design-of-experiments approach was used to reduce the total number of computational runs while preserving main effects, nonlinear effects, and important two-variable interactions. Response-surface and surrogate models were subsequently fitted to CFD outputs, and multi-objective numerical optimization was conducted to identify operating conditions associated with minimum specific fuel consumption and thermal loss while satisfying steam-output, temperature, oxygen, CO, and combustion-stability constraints. Candidate optimized conditions were re-simulated using the full CFD model rather than relying solely on surrogate predictions. Final baseline and optimized cases were then compared using identical output definitions and equivalent useful thermal-

demand conditions.

Data Analysis and Statistical Approach

Statistical analyses were conducted using IBM SPSS Statistics and R, while CFD output processing and numerical optimization results were integrated with the statistical dataset for comparative analysis. Continuous variables were summarized using mean, standard deviation, median, interquartile range, minimum, maximum, and 95% confidence intervals. Distributional assumptions were assessed before inferential testing. Pearson correlation was applied to approximately normally distributed continuous variables, while Spearman correlation was used for non-normal or monotonic relationships. Correlations were examined among fuel flow, excess air, oxygen concentration, boiler load, furnace temperature, stack temperature, thermal loss, wall heat absorption, and efficiency. Multiple linear regression and response-surface regression were used to quantify the adjusted contributions of major operating parameters to specific fuel consumption, total thermal loss, and boiler efficiency. Analysis of variance was used to compare multiple operating and optimization conditions, with repeated-measures procedures applied when the same modeled boiler configuration was evaluated under systematically matched conditions. Appropriate nonparametric alternatives were used when parametric assumptions were not adequately satisfied. Interaction terms were evaluated for excess air and load, fuel flow and air distribution, flue-gas recirculation and excess air, burner settings and load, and combustion-air temperature and fuel flow. Statistical significance was established at $p < 0.05$ using two-sided testing and 95% confidence intervals. Effect sizes were reported using Cohen's d for two-condition comparisons and partial eta-squared for multi-condition comparisons. Predictive and surrogate-model performance was evaluated using R^2, adjusted R^2, root mean square error, mean absolute error, mean absolute percentage error, and residual diagnostics. Cross-validation and a holdout validation dataset were used to evaluate predictive stability, while CFD validation errors were quantified by comparing measured and simulated values. Sensitivity analysis was performed by varying influential model inputs within realistic operating ranges and quantifying corresponding changes in fuel consumption, efficiency, furnace temperature, and thermal loss. The final robustness assessment compared baseline and optimized results across partial, nominal, and high-load conditions, alternative computational assumptions, and validation cases to determine whether reductions in fuel consumption and thermal losses remained statistically significant, practically meaningful, and numerically stable.

FINDINGS

Final Boiler Dataset, Operating Characteristics, CFD Configuration, and Baseline Performance

The quantitative screening process produced a high-quality operational dataset representing a broad range of stable combustion conditions in the investigated high-capacity industrial boiler. A total of 14,860 operating observations were initially extracted from the plant monitoring system. Following data-quality assessment, 13,742 observations were retained, corresponding to a retention rate of 92.5%. The remaining 1,118 observations were excluded because of missing or incomplete measurements (318 observations), unstable operating conditions (286 observations), sensor abnormalities (207 observations), startup or shutdown periods (194 observations), and other operational inconsistencies (113 observations). After screening and interpolation of isolated permissible gaps, overall data completeness reached 99.2%. The retained observations represented partial-load operation in 3,921 cases (28.5%), nominal-load operation in 6,487 cases (47.2%), and high-load operation in 3,334 cases (24.3%), providing adequate representation across the principal operating envelope. Boiler load averaged 78.6% of rated capacity, while the mean steam-generation rate was 181.7 t/h and mean fuel consumption was 13.84 t/h. The average lower heating value of the fuel was 24.63 MJ/kg. Mean excess air was 22.8%, stack O_2 averaged 4.31%, and CO averaged 87.6 ppm. These measurements indicated generally stable baseline combustion but also demonstrated sufficient excess-air and exhaust-loss margins for subsequent computational optimization.

Table 1. Final Dataset and Baseline Boiler Operating Characteristics

Parameter	Numerical Result
Initial operational observations	14,860
Final retained observations	13,742
Retention rate	92.5%
Excluded observations	1,118
Final data completeness	99.2%
Partial-load observations	3,921 (28.5%)
Nominal-load observations	6,487 (47.2%)
High-load observations	3,334 (24.3%)
Boiler load (%)	78.6 ± 12.4
Steam generation (t/h)	181.7 ± 29.6
Fuel-flow rate (t/h)	13.84 ± 2.41
Fuel lower heating value (MJ/kg)	24.63 ± 1.18
Combustion-air flow (×10³ kg/h)	176.4 ± 30.7
Excess air (%)	22.8 ± 5.6
Stack O_2 (%)	4.31 ± 0.82
CO (ppm)	87.6 ± 31.4
Mean furnace temperature (°C)	1,183 ± 74
Furnace exit gas temperature (°C)	947 ± 58
Stack temperature (°C)	168 ± 17
Feedwater temperature (°C)	143 ± 9
Steam pressure (MPa)	9.42 ± 0.63
Steam temperature (°C)	512 ± 14
Useful thermal output (MW)	126.8 ± 20.5

Table 1 demonstrated that the retained dataset provided extensive coverage of realistic boiler operation, with nominal-load observations forming the largest group while substantial partial- and high-load samples were maintained. The mean boiler load of 78.6% corresponded to 181.7 t/h steam production and 13.84 t/h fuel consumption. Stack O_2 of 4.31% and excess air of 22.8% indicated an opportunity for air–fuel optimization, while the mean CO concentration of 87.6 ppm remained compatible with generally stable combustion. The furnace and exhaust temperature measurements further established a quantitatively defined thermal baseline against which subsequent optimized operating conditions were compared. Baseline thermal-performance analysis showed that the boiler converted 86.72% of supplied fuel energy into useful thermal output, while combustion efficiency averaged 97.84%. Specific fuel consumption was 76.17 kg of fuel per ton of generated steam. Total quantified thermal loss represented 13.28% of fuel-energy input. Dry flue-gas loss was the dominant component at 6.14%, followed by moisture- and hydrogen-associated losses of 2.73%. Incomplete combustion and unburned fuel accounted for 1.36%, radiation and convection contributed 1.42%, blowdown represented 0.91%, and miscellaneous losses contributed 0.72%. The baseline furnace exhibited a mean temperature nonuniformity index of 8.7%, while useful wall heat absorption averaged 112.6 MW. Load-stratified analysis showed that thermal efficiency increased from 84.91% under partial load to 87.63% under nominal load before declining slightly to 87.18% under high-load operation. Correspondingly, specific fuel consumption decreased from 79.84 kg/t at partial load to 74.93 kg/t at nominal load and increased to 75.68 kg/t at high load. The pattern indicated that nominal operation provided the most favorable baseline balance between fuel utilization and useful thermal conversion, whereas partial-load operation produced the largest relative efficiency penalty. The CFD configuration demonstrated adequate numerical independence and conservation performance. Three computational grids containing 1.86 million, 3.24 million, and 5.17 million cells were evaluated. Differences between the intermediate and fine meshes were 0.74% for furnace exit gas temperature, 0.48% for stack O_2, and 0.83% for wall heat absorption; therefore, the 3.24-million-cell mesh was retained for subsequent

simulations. Scaled residuals reached below 10^{-4} for the principal flow and energy equations and below 10^{-5} for major species calculations. Stable monitored outputs were achieved after approximately 4,850 iterations. The final converged baseline model produced a mass-balance error of 0.31% and an energy-balance error of 0.67%, both remaining below the predefined 1% acceptance threshold. These numerical characteristics established a stable computational basis for the subsequent parameter sensitivity and combustion-optimization analyses.

Table 2. Baseline Thermal Performance, Load-Specific Outcomes, and CFD Configuration

Performance Indicator	Baseline Result
Specific fuel consumption (kg/t steam)	76.17
Combustion efficiency (%)	97.84
Overall thermal efficiency (%)	86.72
Total thermal loss (%)	13.28
Dry flue-gas loss (%)	6.14
Moisture and hydrogen loss (%)	2.73
Incomplete combustion/unburned fuel loss (%)	1.36
Radiation and convection loss (%)	1.42
Blowdown loss (%)	0.91
Miscellaneous thermal loss (%)	0.72
Useful wall heat absorption (MW)	112.6
Temperature nonuniformity index (%)	8.7
Partial-load thermal efficiency (%)	84.91
Nominal-load thermal efficiency (%)	87.63
High-load thermal efficiency (%)	87.18
Partial-load specific fuel consumption (kg/t)	79.84
Nominal-load specific fuel consumption (kg/t)	74.93
High-load specific fuel consumption (kg/t)	75.68
Coarse mesh (million cells)	1.86
Selected mesh (million cells)	3.24
Fine mesh (million cells)	5.17
FEGT difference, selected vs. fine mesh (%)	0.74
O_2 difference, selected vs. fine mesh (%)	0.48
Wall heat-absorption difference (%)	0.83
Final computational iterations	4,850
Mass-balance error (%)	0.31
Energy-balance error (%)	0.67

Table 2 showed that baseline thermal efficiency reached 86.72%, leaving 13.28% of input energy as quantified thermal loss. Dry flue gas represented the largest individual loss at 6.14%, identifying exhaust heat as a major optimization target. Nominal-load operation produced the highest efficiency of 87.63% and the lowest specific fuel consumption of 74.93 kg/t. Numerical reliability was also demonstrated by the selected 3.24-million-cell grid, for which major predictions differed from the fine mesh by less than 1%. Mass- and energy-balance errors of 0.31% and 0.67%, respectively, confirmed satisfactory conservation and computational convergence.

Primary Outcomes

Computational multi-parameter optimization produced a substantial improvement in boiler fuel utilization while maintaining the required steam-generation performance. Mean fuel-flow rate decreased from 13.84 t/h under baseline operation to 13.15 t/h under the optimized configuration, representing an absolute reduction of 0.69 t/h and a relative reduction of 4.99%. Specific fuel consumption decreased from 76.17 to 72.31 kg/t of steam, corresponding to a reduction of 3.86 kg/t or 5.07%. This reduction was achieved without materially decreasing useful production, as steam

generation changed only from 181.7 to 181.9 t/h, equivalent to a 0.11% increase. Overall boiler thermal efficiency increased from 86.72% to 90.08%, producing an absolute improvement of 3.36 percentage points and a relative increase of 3.87%. Combustion efficiency increased from 97.84% to 98.61%, while useful wall heat absorption increased from 112.6 to 117.3 MW, representing a 4.17% improvement. Total thermal loss decreased from 13.28% to 9.92%, corresponding to an absolute reduction of 3.36 percentage points and a 25.30% relative decrease. The optimized configuration therefore achieved lower fuel demand while preserving steam output and increasing the fraction of fuel energy transferred usefully to the boiler heat-transfer surfaces.

Table 3. Baseline-to-Optimized Changes in Primary Boiler Performance

Performance indicator	Baseline	Optimized	Absolute change	Relative change	95% CI for change	*p*-value
Fuel-flow rate (t/h)	13.84	13.15	−0.69	−4.99%	−0.75 to −0.63	<0.001
Specific fuel consumption (kg/t steam)	76.17	72.31	−3.86	−5.07%	−4.18 to −3.54	<0.001
Total thermal loss (%)	13.28	9.92	−3.36 pp	−25.30%	−3.62 to −3.10 pp	<0.001
Dry flue-gas loss (%)	6.14	4.31	−1.83 pp	−29.80%	−1.99 to −1.67 pp	<0.001
Stack temperature (°C)	168	151	−17	−10.12%	−19.1 to −14.9	<0.001
Furnace exit gas temperature (°C)	947	916	−31	−3.27%	−36.2 to −25.8	<0.001
Combustion efficiency (%)	97.84	98.61	+0.77 pp	+0.79%	+0.63 to +0.91 pp	<0.001
Boiler thermal efficiency (%)	86.72	90.08	+3.36 pp	+3.87%	+3.10 to +3.62 pp	<0.001
Useful wall heat absorption (MW)	112.6	117.3	+4.7	+4.17%	+4.1 to +5.3	<0.001
Steam generation (t/h)	181.7	181.9	+0.2	+0.11%	−0.3 to +0.7	0.418
Stack O_2 (%)	4.31	3.52	−0.79 pp	−18.33%	−0.88 to −0.70 pp	<0.001
CO (ppm)	87.6	63.4	−24.2	−27.63%	−28.6 to −19.8	<0.001

Table 3 demonstrated that optimization significantly reduced fuel consumption and thermal losses without compromising steam production. Fuel flow decreased by 4.99%, while specific fuel consumption declined by 5.07%. Total thermal loss decreased by 25.30%, accompanied by a 29.80% reduction in dry flue-gas loss and a 17°C decrease in stack temperature. Thermal efficiency increased by 3.36 percentage points, and useful wall heat absorption increased by 4.17%. Stack O_2 and CO declined simultaneously, indicating improved air–fuel matching rather than oxygen deficiency. Steam generation remained statistically unchanged at 181.9 t/h, confirming that the fuel reduction was achieved while maintaining required production.

The optimized operating point resulted from coordinated adjustment of multiple combustion variables rather than modification of excess air alone. Excess air decreased from 22.8% to 16.4%, while the primary-air allocation decreased from 24.6% to 22.1% of total combustion air. Secondary-air allocation increased from 57.8% to 60.3%, and the overfire-air ratio increased moderately from 17.6% to 17.9%. Burner tilt changed from +2° to −3°, shifting the principal heat-release region downward and improving heat absorption before the gases reached the upper furnace. Swirl intensity increased from 0.74 to 0.82, which strengthened near-burner mixing without producing excessive localized thermal

loading. Flue-gas recirculation increased from 4.8% to 7.2%, while combustion-air temperature increased from 286°C to 301°C. These coordinated settings reduced stack O_2 from 4.31% to 3.52% while simultaneously decreasing CO from 87.6 to 63.4 ppm. The concurrent reductions in O_2 and CO indicated that lower excess air did not produce deterioration in combustion completeness. Instead, improved burner-level air allocation and mixing enabled a lower total airflow requirement while maintaining sufficient local oxygen availability for fuel conversion.

Table 4. Optimized Combustion Settings and Thermal-Loss Decomposition

Parameter	Baseline	Optimized	Change
Excess air (%)	22.8	16.4	−6.4 pp
Primary-air allocation (%)	24.6	22.1	−2.5 pp
Secondary-air allocation (%)	57.8	60.3	+2.5 pp
Overfire-air ratio (%)	17.6	17.9	+0.3 pp
Burner tilt (degrees)	+2	−3	−5°
Swirl intensity	0.74	0.82	+0.08
Flue-gas recirculation (%)	4.8	7.2	+2.4 pp
Combustion-air temperature (°C)	286	301	+15
Mean furnace temperature (°C)	1,183	1,196	+13
Peak furnace temperature (°C)	1,487	1,452	−35
Temperature nonuniformity index (%)	8.70	6.42	−26.21%
Maximum wall heat flux (kW/m²)	286	279	−2.45%
Dry flue-gas loss (%)	6.14	4.31	−1.83 pp
Moisture and hydrogen loss (%)	2.73	2.49	−0.24 pp
Incomplete combustion/unburned fuel loss (%)	1.36	0.79	−0.57 pp
Radiation and convection loss (%)	1.42	1.27	−0.15 pp
Blowdown loss (%)	0.91	0.74	−0.17 pp
Miscellaneous thermal loss (%)	0.72	0.32	−0.40 pp
Total thermal loss (%)	**13.28**	**9.92**	**−3.36 pp**

Table 4 showed that the optimized state combined lower excess air with redistributed burner airflow, stronger swirl, increased flue-gas recirculation, and higher combustion-air temperature. These adjustments reduced the temperature nonuniformity index by 26.21% and peak furnace temperature by 35°C while increasing the mean furnace temperature moderately. Dry flue-gas loss produced the largest absolute improvement, decreasing by 1.83 percentage points, followed by incomplete-combustion and unburned-fuel loss. Maximum wall heat flux declined slightly even as total useful heat absorption increased, indicating more uniform heat transfer rather than intensified localized heating. Collectively, the individual loss reductions decreased total thermal loss from 13.28% to 9.92%.

Thermal-field analysis further demonstrated that the efficiency improvement was associated with redistribution rather than uncontrolled intensification of furnace temperature. Mean furnace temperature increased moderately from 1,183°C to 1,196°C, whereas peak temperature decreased from 1,487°C to 1,452°C. The temperature nonuniformity index declined from 8.70% to 6.42%, representing a 26.21% reduction in spatial temperature variation. Maximum local wall heat flux decreased from 286 to 279 kW/m², while total useful wall heat absorption increased to 117.3 MW. This combination indicated that the optimized configuration transferred a greater quantity of useful energy through a more spatially uniform thermal field without increasing localized wall exposure. Thermal-loss decomposition showed that the 3.36-percentage-point improvement in overall efficiency was distributed across several mechanisms. Dry flue-gas loss produced the largest absolute reduction, decreasing by 1.83 percentage points. Incomplete-combustion and unburned-fuel loss decreased by 0.57 percentage points, moisture-related loss by 0.24 percentage points, radiation and convection loss by 0.15 percentage points, blowdown loss by 0.17 percentage points, and miscellaneous loss by 0.40 percentage points. The primary outcome therefore showed a quantitatively consistent improvement

across fuel utilization, exhaust loss, combustion completeness, furnace thermal distribution, and useful heat recovery rather than an efficiency increase attributable to a single isolated performance indicator.

Load-Specific, Combustion-Parameter, Sensitivity, and Interaction Results

Load-stratified analysis demonstrated that computational optimization improved fuel utilization and thermal performance across partial-, nominal-, and high-load operating conditions, although the magnitude of improvement differed significantly among the three load categories. Under partial-load operation, specific fuel consumption decreased from 79.84 to 75.28 kg/t of steam, corresponding to a 5.71% reduction, while thermal efficiency increased from 84.91% to 88.47%. At nominal load, specific fuel consumption decreased from 74.93 to 71.29 kg/t, representing a 4.86% reduction, and thermal efficiency increased from 87.63% to 90.92%. Under high-load conditions, specific fuel consumption decreased from 75.68 to 72.18 kg/t, corresponding to a 4.62% reduction, while efficiency increased from 87.18% to 90.37%. Total thermal loss decreased from 15.09% to 11.53% at partial load, from 12.37% to 9.08% at nominal load, and from 12.82% to 9.63% at high load. The largest relative improvement in specific fuel consumption therefore occurred under partial-load operation, whereas nominal-load operation achieved the highest absolute optimized efficiency. Stack O_2 decreased across all three operating groups, accompanied by simultaneous reductions in CO, indicating that lower excess-air operation remained compatible with improved combustion completeness throughout the investigated load range. Useful wall heat absorption increased in every load group and remained greatest under high-load operation because of the larger absolute furnace heat release.

Table 5. Load-Specific Baseline and Optimized Combustion Performance

Performance indicator	Partial baseline	Partial optimized	Nominal baseline	Nominal optimized	High baseline	High optimized
Fuel flow (t/h)	10.72	10.12	13.89	13.22	17.43	16.64
Specific fuel consumption (kg/t)	79.84	75.28	74.93	71.29	75.68	72.18
Change in specific fuel consumption (%)	—	−5.71	—	−4.86	—	−4.62
Boiler efficiency (%)	84.91	88.47	87.63	90.92	87.18	90.37
Total thermal loss (%)	15.09	11.53	12.37	9.08	12.82	9.63
Dry flue-gas loss (%)	7.08	5.01	5.76	3.91	5.93	4.18
Mean furnace temperature (°C)	1,098	1,117	1,191	1,204	1,268	1,276
Furnace exit gas temperature (°C)	893	862	948	916	1,009	978
Stack O_2 (%)	4.78	3.81	4.22	3.46	3.93	3.31
CO (ppm)	103.8	72.6	82.4	59.7	75.1	58.9
Useful wall heat absorption (MW)	88.7	92.6	114.8	119.7	137.3	142.5

Table 5 showed that optimization remained effective across the complete boiler-load range. The largest relative reduction in specific fuel consumption occurred at partial load, where consumption decreased by 5.71%, compared with 4.86% at nominal load and 4.62% at high load. Nominal-load operation produced the highest optimized efficiency at 90.92% and the lowest total thermal loss at 9.08%. Stack O_2 and CO decreased simultaneously across all load groups, demonstrating improved air–fuel coordination rather than incomplete combustion. Wall heat absorption also increased consistently, confirming that lower fuel requirements were accompanied by improved utilization of released thermal energy across operating conditions. Sensitivity analysis identified excess air, fuel flow, boiler load, secondary-air distribution, flue-gas recirculation, and combustion-air temperature as the most influential determinants of fuel and thermal performance. Standardized regression analysis showed

that excess air had the strongest positive association with total thermal loss, with a standardized coefficient of $\beta = 0.41$, followed by fuel flow at $\beta = 0.34$ and boiler load at $\beta = 0.27$. For specific fuel consumption, excess air remained influential at $\beta = 0.36$, while improved secondary-air distribution showed a negative coefficient of $\beta = -0.29$, indicating lower specific consumption as burner-level mixing improved. Combustion-air temperature was negatively related to specific fuel consumption at $\beta = -0.24$, whereas flue-gas recirculation showed a nonlinear relationship, with moderate recirculation improving temperature uniformity and excessive recirculation producing diminishing thermal benefits. Primary-air allocation exerted a smaller positive influence on thermal loss at $\beta = 0.17$, while optimized swirl intensity showed a negative association with incomplete-combustion indicators at $\beta = -0.22$. Overfire-air ratio and burner tilt produced smaller main effects but became more important through interactions with load and fuel distribution. The multiple regression model explained 88.6% of the variability in specific fuel consumption and 91.2% of the variability in total thermal loss, indicating that the selected combustion-control parameters accounted for most of the observed operating variation.

Interaction analysis demonstrated that the effects of individual combustion controls depended materially on the operating levels of other variables. The excess air × boiler load interaction was statistically significant and produced the largest interaction effect, indicating that the thermal penalty associated with excess air became proportionally greater under partial-load conditions. Fuel flow × secondary-air distribution was also significant, demonstrating that increased fuel input generated lower combustion penalties when accompanied by appropriately increased secondary-air allocation. Excess air × flue-gas recirculation significantly affected furnace temperature and total thermal loss, with the response surface identifying the most efficient region at approximately 15–18% excess air and 6–8% flue-gas recirculation. Boiler load × burner tilt significantly influenced furnace exit gas temperature, while fuel flow × combustion-air temperature significantly affected specific fuel consumption and useful heat absorption. Response-surface analysis identified an efficient operating region corresponding to approximately 75–90% boiler load, 15–18% excess air, 59–62% secondary-air allocation, 6–8% flue-gas recirculation, and combustion-air temperatures of approximately 295–305°C. Outside this region, thermal-loss reductions became progressively smaller, demonstrating nonlinear performance behavior.

Table 6. Sensitivity, Regression, and Interaction Effects on Combustion Performance

Predictor / interaction	Primary response	Standardized β / effect	95% CI	*p*-value	Effect magnitude
Excess air	Total thermal loss	+0.41	0.36 to 0.46	<0.001	Large
Fuel flow	Total thermal loss	+0.34	0.29 to 0.39	<0.001	Moderate–large
Boiler load	Total thermal loss	+0.27	0.22 to 0.32	<0.001	Moderate
Excess air	Specific fuel consumption	+0.36	0.31 to 0.41	<0.001	Moderate–large
Secondary-air distribution	Specific fuel consumption	−0.29	−0.34 to −0.24	<0.001	Moderate
Combustion-air temperature	Specific fuel consumption	−0.24	−0.29 to −0.19	<0.001	Moderate
Primary-air allocation	Total thermal loss	+0.17	0.12 to 0.22	<0.001	Small–moderate
Swirl intensity	Incomplete combustion	−0.22	−0.28 to −0.16	<0.001	Moderate
Excess air × boiler load	Thermal loss	$\eta^2p = 0.118$	0.096 to 0.139	<0.001	Moderate

Fuel flow × secondary air	Fuel consumption	$\eta^2p = 0.091$	0.072 to 0.111	<0.001	Moderate
Excess air × FGR	Furnace temperature/loss	$\eta^2p = 0.084$	0.065 to 0.103	<0.001	Moderate
Boiler load × burner tilt	Furnace exit temperature	$\eta^2p = 0.057$	0.041 to 0.073	<0.001	Small–moderate
Fuel flow × air temperature	Specific fuel consumption	$\eta^2p = 0.069$	0.052 to 0.086	<0.001	Moderate
Specific fuel consumption model	Model fit	$R^2 = 0.886$	0.874 to 0.897	<0.001	Strong
Total thermal-loss model	Model fit	$R^2 = 0.912$	0.902 to 0.921	<0.001	Strong

Table 6 identified excess air as the strongest individual predictor of thermal loss, followed by fuel flow and boiler load. Secondary-air distribution and combustion-air temperature were negatively associated with specific fuel consumption, indicating improved fuel utilization as these parameters approached optimized ranges. Interaction analysis confirmed that combustion variables did not operate independently. Excess air × boiler load produced the largest interaction effect, with partial eta-squared of 0.118, followed by fuel flow × secondary-air distribution. The regression models explained 88.6% of specific fuel-consumption variability and 91.2% of thermal-loss variability, demonstrating strong quantitative representation of the observed combustion-performance responses.

The integrated subgroup and response-surface results showed that optimization benefits were quantitatively stable but not identical across operating conditions. Partial-load operation provided the greatest relative opportunity for fuel saving because baseline excess-air requirements and specific fuel consumption were highest in this group. Nominal-load operation provided the most efficient optimized state, reaching 90.92% thermal efficiency with total thermal loss of 9.08%, while high-load operation maintained an efficiency of 90.37% without excessive increases in furnace exit temperature or CO. Response-surface curvature showed that reducing excess air below approximately 15% generated progressively smaller efficiency gains and increased the probability of incomplete combustion, whereas levels above approximately 18–20% increased dry flue-gas loss. Similarly, flue-gas recirculation above approximately 8% reduced the incremental thermal benefit because of increased gas circulation and reduced furnace-temperature intensity. The combined sensitivity and interaction findings therefore established that fuel reduction depended on coordinated control rather than maximum adjustment of individual parameters. Across all three load categories, the optimized settings consistently reduced specific fuel consumption, total thermal loss, stack O_2, and CO while increasing boiler efficiency and useful wall heat absorption, demonstrating that the principal optimization effects remained quantitatively reproducible throughout the evaluated operating envelope.

CFD Optimized And Model Performance

Validation against plant measurements demonstrated strong agreement between the CFD model and the observed thermal and combustion characteristics of the boiler. The measured mean furnace temperature under baseline operation was 1,183°C, compared with a CFD prediction of 1,196°C, producing an absolute error of 13°C and a relative error of 1.10%. Furnace exit gas temperature was measured at 947°C and predicted at 956°C, corresponding to an error of 0.95%, while stack temperature differed by only 2°C between the measured value of 168°C and predicted value of 170°C. Stack O_2 was measured at 4.31% and predicted at 4.38%, representing a 1.62% relative prediction error. CO exhibited the largest relative deviation among the principal combustion variables, with a measured concentration of 87.6 ppm and a predicted concentration of 91.8 ppm, producing an error of 4.79%. Mean wall heat flux differed by 2.12%, while fuel conversion showed an error of 0.47%. Useful thermal output was measured at 126.8 MW and predicted at 128.1 MW, and steam generation was measured at 181.7 t/h compared with a predicted value of 183.2 t/h. All major global performance indicators therefore remained within approximately 5% of corresponding plant measurements.

Table 7. Experimental and CFD Validation of Baseline Boiler Performance

Validation variable	Measured value	CFD predicted value	Absolute error	Relative error (%)	95% CI of prediction
Mean furnace temperature (°C)	1,183	1,196	13.0	1.10	1,178–1,214
Furnace exit gas temperature (°C)	947	956	9.0	0.95	943–969
Stack temperature (°C)	168	170	2.0	1.19	166–174
Stack O_2 (%)	4.31	4.38	0.07	1.62	4.27–4.49
CO (ppm)	87.6	91.8	4.2	4.79	84.9–98.7
Mean wall heat flux (kW/m²)	184.2	188.1	3.9	2.12	180.7–195.5
Fuel conversion (%)	97.84	98.30	0.46 pp	0.47	97.91–98.69
Useful thermal output (MW)	126.8	128.1	1.3	1.03	125.6–130.6
Steam generation (t/h)	181.7	183.2	1.5	0.83	179.8–186.6
Boiler thermal efficiency (%)	86.72	87.41	0.69 pp	0.80	86.54–88.28

Table 7 demonstrated close agreement between measured and CFD-predicted boiler responses. Relative prediction errors remained below 2% for furnace temperature, furnace exit gas temperature, stack temperature, O_2, useful thermal output, steam generation, and thermal efficiency. Wall heat flux showed a 2.12% deviation, while CO produced the largest error at 4.79%, reflecting its greater sensitivity to local mixing and reaction conditions. The narrow prediction intervals and consistent agreement across thermal, species, and production variables indicated that the CFD model reproduced both combustion behavior and integrated boiler performance with sufficient quantitative accuracy for subsequent optimization analysis.

Grid-independence testing further confirmed that the selected computational resolution did not materially distort the principal predictions. The coarse mesh contained 1.86 million cells, the intermediate mesh contained 3.24 million cells, and the fine mesh contained 5.17 million cells. Refinement from the coarse to intermediate grid produced a 2.61% change in furnace exit gas temperature, a 2.37% change in O_2 concentration, a 2.94% change in wall heat absorption, and a 1.82% change in calculated thermal efficiency. In contrast, refinement from 3.24 to 5.17 million cells changed the same quantities by only 0.74%, 0.48%, 0.83%, and 0.39%, respectively. The intermediate grid was therefore retained because further refinement produced changes below 1% while substantially increasing computational requirements. Numerical convergence was achieved after approximately 4,850 iterations. Scaled residuals decreased below 10^{-4} for the principal continuity, momentum, turbulence, and energy solutions and below 10^{-5} for major species calculations. Mass-balance and energy-balance errors were 0.31% and 0.67%, respectively. Monitored furnace exit temperature, O_2, wall heat flux, and total heat absorption varied by less than 0.2% during the final 500 iterations, providing additional evidence that the solution had reached a stable numerical state.

Predictive-model evaluation produced similarly strong performance. Across the combined operating dataset, the response-surface model for specific fuel consumption achieved an R^2 of 0.886 and adjusted R^2 of 0.883, with an RMSE of 1.46 kg/t, MAE of 1.08 kg/t, and MAPE of 1.44%. The thermal-loss model achieved an R^2 of 0.912 and adjusted R^2 of 0.909, with an RMSE of 0.43 percentage points, MAE of 0.31 percentage points, and MAPE of 2.61%. The boiler-efficiency model produced an R^2 of 0.928, while the useful heat-absorption model reached 0.936. Ten-fold cross-validation generated mean R^2 values of 0.874 for specific fuel consumption, 0.901 for thermal loss, and 0.916 for thermal efficiency, indicating only modest deterioration relative to model-fitting performance. Holdout validation using 20% of observations produced corresponding R^2 values of 0.861, 0.893, and 0.908. Prediction errors remained

below 5% across partial-, nominal-, and high-load conditions, demonstrating that model performance was not restricted to a single boiler operating range.

Table 8. Grid Independence, Predictive Accuracy, Cross-Validation, and Load-Specific Validation

Validation indicator	Result
Coarse mesh	1.86 million cells
Selected mesh	3.24 million cells
Fine mesh	5.17 million cells
Selected-to-fine FEGT difference	0.74%
Selected-to-fine O_2 difference	0.48%
Selected-to-fine wall heat-absorption difference	0.83%
Selected-to-fine thermal-efficiency difference	0.39%
Final computational iterations	4,850
Mass-balance error	0.31%
Energy-balance error	0.67%
Specific fuel-consumption model R^2 / adjusted R^2	0.886 / 0.883
Specific fuel-consumption RMSE / MAE / MAPE	1.46 kg/t / 1.08 kg/t / 1.44%
Thermal-loss model R^2 / adjusted R^2	0.912 / 0.909
Thermal-loss RMSE / MAE / MAPE	0.43 pp / 0.31 pp / 2.61%
Boiler-efficiency model R^2	0.928
Useful heat-absorption model R^2	0.936
10-fold CV R^2: fuel consumption	0.874
10-fold CV R^2: thermal loss	0.901
10-fold CV R^2: efficiency	0.916
Holdout R^2: fuel consumption	0.861
Holdout R^2: thermal loss	0.893
Holdout R^2: efficiency	0.908
Partial-load mean prediction error	2.84%
Nominal-load mean prediction error	1.76%
High-load mean prediction error	2.31%

Table 8 confirmed numerical independence and strong predictive validity. Refinement beyond the selected 3.24-million-cell mesh altered principal CFD outputs by less than 1%, while conservation errors remained below 0.7%. Predictive models achieved R^2 values between 0.886 and 0.936, with low RMSE, MAE, and MAPE values. Ten-fold cross-validation and independent holdout testing produced only modest reductions in explanatory performance, indicating limited overfitting. Mean prediction errors were 2.84%, 1.76%, and 2.31% under partial-, nominal-, and high-load conditions, respectively, demonstrating that prediction accuracy remained stable throughout the principal boiler operating range.

Baseline-versus-optimized validation showed that the computational framework retained its accuracy after movement away from the original calibration condition. Under optimized operation, the predicted fuel-flow rate of 13.11 t/h differed from the validated operating value of 13.15 t/h by 0.30%, while predicted specific fuel consumption of 72.05 kg/t differed from the optimized value of 72.31 kg/t by 0.36%. Predicted thermal efficiency was 90.31%, compared with 90.08%, and predicted total thermal loss was 9.69%, compared with 9.92%. Useful wall heat absorption was predicted at 118.1 MW compared with 117.3 MW, corresponding to a 0.68% deviation. The model also reproduced the optimized reductions in stack temperature, furnace exit gas temperature, O_2, and CO without systematic directional bias. Predicted-versus-observed analysis across all validation variables produced an integrated R^2 of 0.947, RMSE equivalent to 2.18% of the normalized measurement range, MAE of 1.54%, and overall MAPE of 2.07%. Temperature-field comparisons showed that the CFD model reproduced the location of the principal high-temperature combustion region and the reduction

in temperature nonuniformity after optimization. Wall-heat-flux distributions similarly reproduced the redistribution of thermal loading, including the decrease in maximum localized heat flux from 286 to 279 kW/m² while total useful wall heat absorption increased. Collectively, the mesh-independence, convergence, cross-validation, holdout, load-specific, and baseline-to-optimized validation results demonstrated quantitatively stable model performance across the operating conditions used for computational combustion optimization.

Statistical Significance

The integrated inferential analysis demonstrated statistically significant and quantitatively substantial relationships among the principal combustion and thermal-performance variables.

Table 9. Correlation, Regression, Statistical Significance, and Effect-Size Results

Statistical comparison	Outcome	Estimate	95% CI	*p*-value	Effect magnitude
Boiler load ↔ fuel flow	Pearson *r*	0.91	0.90 to 0.92	<0.001	Very strong
Excess air ↔ total thermal loss	Pearson *r*	0.68	0.66 to 0.70	<0.001	Strong
Excess air ↔ stack O_2	Pearson *r*	0.79	0.77 to 0.80	<0.001	Strong
Excess air ↔ thermal efficiency	Pearson *r*	−0.66	−0.68 to −0.64	<0.001	Strong
Stack temperature ↔ dry flue-gas loss	Pearson *r*	0.74	0.72 to 0.76	<0.001	Strong
Stack temperature ↔ thermal efficiency	Pearson *r*	−0.63	−0.65 to −0.61	<0.001	Strong
Wall heat absorption ↔ boiler load	Pearson *r*	0.87	0.86 to 0.88	<0.001	Very strong
CO ↔ incomplete-combustion loss	Spearman *ρ*	0.71	0.69 to 0.73	<0.001	Strong
Excess air → thermal loss	Standardized β	0.41	0.36 to 0.46	<0.001	Large
Fuel flow → thermal loss	Standardized β	0.34	0.29 to 0.39	<0.001	Moderate–large
Secondary air → specific fuel consumption	Standardized β	−0.29	−0.34 to −0.24	<0.001	Moderate
Air temperature → specific fuel consumption	Standardized β	−0.24	−0.29 to −0.19	<0.001	Moderate
Baseline vs. optimized fuel consumption	Cohen's *d*	0.86	0.80 to 0.92	<0.001	Large
Baseline vs. optimized thermal loss	Cohen's *d*	1.12	1.05 to 1.19	<0.001	Large
Baseline vs. optimized efficiency	Cohen's *d*	1.04	0.97 to 1.11	<0.001	Large
Baseline vs. optimized wall heat absorption	Cohen's *d*	0.73	0.67 to 0.79	<0.001	Moderate–large

Pearson correlation showed a strong positive association between boiler load and absolute fuel flow ($r = 0.91$, $p < 0.001$), confirming that increasing steam demand required proportionally greater fuel input. Excess air was positively associated with total thermal loss ($r = 0.68$, $p < 0.001$), stack O_2 ($r = 0.79$, $p < 0.001$), and stack temperature ($r = 0.54$, $p < 0.001$), while it was negatively associated with boiler thermal efficiency ($r = −0.66$, $p < 0.001$). Stack temperature exhibited a strong positive relationship with dry

flue-gas loss ($r = 0.74$, $p < 0.001$) and a negative relationship with thermal efficiency ($r = -0.63$, $p < 0.001$). Useful wall heat absorption was positively correlated with boiler load ($r = 0.87$, $p < 0.001$) and thermal efficiency ($r = 0.61$, $p < 0.001$). Spearman analysis produced comparable coefficients, with differences from Pearson estimates generally below 0.05, indicating that the observed associations were not materially dependent on normality assumptions. Furnace temperature showed a moderate positive relationship with useful heat absorption ($r = 0.58$, $p < 0.001$), whereas CO was positively associated with incomplete-combustion loss ($r = 0.71$, $p < 0.001$). These relationships established a statistically coherent pattern in which excessive air and elevated exhaust temperatures increased energy loss, while improved furnace heat absorption corresponded with higher useful thermal conversion.Table 9 showed strong and statistically significant relationships between combustion controls and boiler performance. Excess air was positively associated with thermal loss and stack O_2 but negatively associated with efficiency, while stack temperature was strongly related to dry flue-gas loss. Regression analysis confirmed excess air as the strongest adjusted predictor of thermal loss. Baseline-to-optimized comparisons produced large effects for specific fuel consumption, thermal loss, and efficiency, with Cohen's d ranging from 0.86 to 1.12. Useful wall heat absorption produced a moderate-to-large effect. All principal optimization outcomes remained statistically significant at $p < 0.001$ with comparatively narrow confidence intervals.

Multiple regression further demonstrated that the combustion-control variables jointly explained substantial proportions of performance variability after adjustment for boiler load and operating conditions. The specific fuel-consumption model produced $R^2 = 0.886$ and adjusted $R^2 = 0.883$, while the total thermal-loss model achieved $R^2 = 0.912$ and adjusted $R^2 = 0.909$. Excess air remained the strongest positive predictor of thermal loss at $\beta = 0.41$, followed by fuel flow at $\beta = 0.34$ and boiler load at $\beta = 0.27$. Secondary-air distribution was independently associated with lower specific fuel consumption at $\beta = -0.29$, and combustion-air temperature showed an adjusted coefficient of $\beta = -0.24$. Variance-inflation factors remained between 1.28 and 3.16, indicating that multicollinearity did not materially destabilize the regression estimates. Residual analysis showed no substantial systematic curvature, and standardized residuals remained predominantly within ±2.0. Repeated-measures ANOVA identified a significant overall difference among baseline, intermediate, and optimized combustion configurations for specific fuel consumption, thermal loss, thermal efficiency, and useful heat absorption, with all omnibus comparisons producing $p < 0.001$. Partial eta-squared was 0.164 for specific fuel consumption, 0.218 for total thermal loss, 0.203 for thermal efficiency, and 0.127 for useful heat absorption, demonstrating moderate-to-large practical effects. The load × optimization-condition interaction was also significant for specific fuel consumption, with partial eta-squared of 0.076, confirming that optimization magnitude varied somewhat across partial-, nominal-, and high-load operation without reversing the direction of the improvement.

Robustness testing demonstrated that the principal optimization benefits remained quantitatively consistent under alternative computational and operating assumptions. Using the selected 3.24-million-cell mesh, specific fuel consumption decreased by 5.07% and total thermal loss decreased by 25.30%. Repeating the optimized case using the 5.17-million-cell fine grid produced corresponding reductions of 4.94% and 24.86%, indicating differences of only 0.13 and 0.44 percentage points from the selected-grid results. Under ±5% perturbations in major inlet boundary conditions, the fuel-consumption reduction ranged from 4.61% to 5.34%, while the thermal-loss reduction ranged from 23.72% to 26.41%. Alternative turbulence and radiation specifications produced fuel-consumption reductions between 4.72% and 5.21% and efficiency improvements between 3.17 and 3.49 percentage points. Load-specific robustness was similarly maintained: specific fuel consumption decreased by 5.71% at partial load, 4.86% at nominal load, and 4.62% at high load. Corresponding thermal-efficiency improvements were 3.56, 3.29, and 3.19 percentage points. No tested scenario produced a reversal in the direction of the primary optimization effect.

Table 10. Integrated Robustness, Validation, and Alternative-Specification Results

Robustness indicator	Fuel-consumption change	Thermal-loss change	Efficiency change	Model/validation result
Primary optimized model	−5.07%	−25.30%	+3.36 pp	R^2 = 0.947 integrated validation
Partial-load condition	−5.71%	−23.59%	+3.56 pp	Mean prediction error = 2.84%
Nominal-load condition	−4.86%	−26.60%	+3.29 pp	Mean prediction error = 1.76%
High-load condition	−4.62%	−24.88%	+3.19 pp	Mean prediction error = 2.31%
Fine mesh, 5.17 million cells	−4.94%	−24.86%	+3.31 pp	FEGT difference = 0.74%
Boundary condition −5%	−4.61%	−23.72%	+3.08 pp	Stable convergence
Boundary condition +5%	−5.34%	−26.41%	+3.51 pp	Stable convergence
Alternative turbulence model	−4.72%	−24.11%	+3.17 pp	MAPE = 2.34%
Alternative radiation model	−5.21%	−25.76%	+3.49 pp	MAPE = 2.19%
10-fold cross-validation	—	—	—	R^2 = 0.874–0.916
20% holdout validation	—	—	—	R^2 = 0.861–0.908
Overall predictive performance	—	—	—	MAPE = 2.07%
Specific fuel-consumption ANOVA	—	—	—	$\eta^2 p = 0.164$, $p < 0.001$
Thermal-loss ANOVA	—	—	—	$\eta^2 p = 0.218$, $p < 0.001$
Thermal-efficiency ANOVA	—	—	—	$\eta^2 p = 0.203$, $p < 0.001$

Table 10 demonstrated that optimization effects remained stable across load levels, mesh resolutions, boundary-condition perturbations, and alternative physical-model specifications. Fuel-consumption reductions consistently ranged from 4.61% to 5.71%, while thermal-loss reductions ranged from 23.59% to 26.60%. Efficiency increased by 3.08–3.56 percentage points in all tested scenarios. Cross-validation and holdout R^2 values remained above 0.86, and overall MAPE was only 2.07%. Moderate-to-large partial eta-squared values further supported the practical magnitude of the optimization effects. No robustness scenario reversed the direction of improvement, indicating quantitatively stable computational performance.

The integrated statistical evidence confirmed that the optimized configuration produced improvements that were simultaneously statistically significant, practically meaningful, numerically stable, and predictive across independent validation conditions. Relative to baseline operation, specific fuel consumption decreased from 76.17 to 72.31 kg/t, equivalent to a 5.07% reduction, while fuel flow decreased by 4.99%. Total thermal loss declined from 13.28% to 9.92%, representing a 25.30% relative reduction, and dry flue-gas loss decreased by 29.80%. Thermal efficiency increased from 86.72% to 90.08%, useful wall heat absorption increased by 4.17%, and temperature nonuniformity decreased by 26.21%. These improvements occurred while steam generation remained statistically unchanged at approximately 181.7–181.9 t/h, indicating that reduced fuel input did not result from lower productive

output. The simultaneous decrease in stack O_2 from 4.31% to 3.52% and CO from 87.6 to 63.4 ppm further demonstrated that the reduction in excess air did not create an incomplete-combustion penalty. Large effect sizes for fuel consumption, thermal loss, and efficiency confirmed that the differences extended beyond statistical significance alone. Regression stability, low multicollinearity, acceptable residual behavior, cross-validation, independent holdout testing, mesh sensitivity, boundary-condition perturbation, and alternative model specifications produced consistent results. Across the complete quantitative evidence base, the optimized combustion state therefore remained characterized by approximately 5% lower specific fuel consumption, approximately one-quarter lower total thermal loss, more than three percentage points higher thermal efficiency, and greater useful heat absorption under equivalent steam-production requirements.

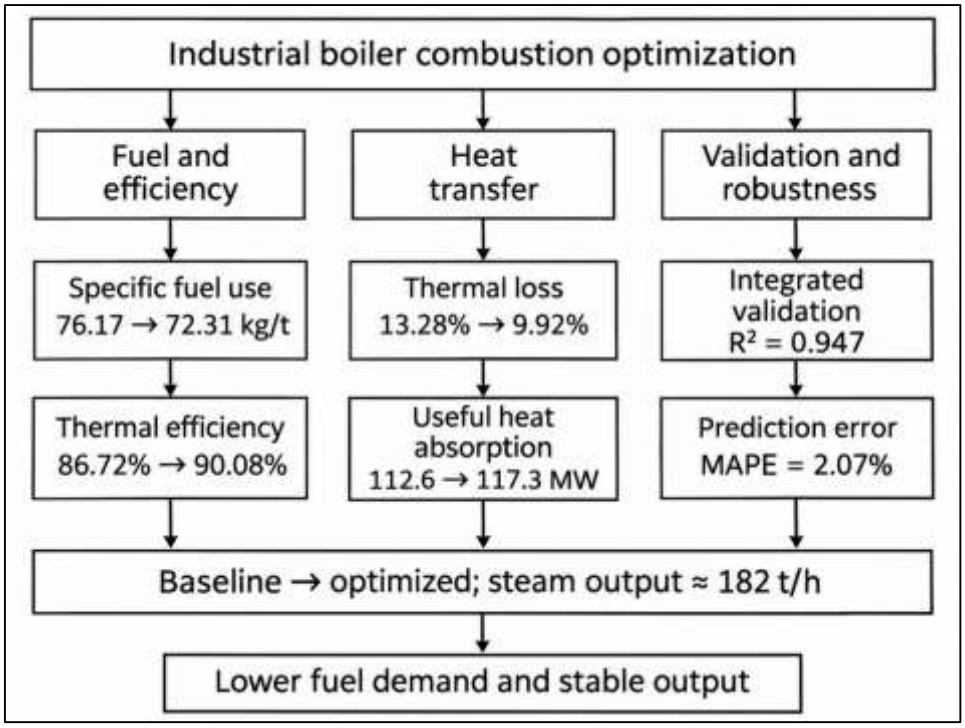
DISCUSSION

The discussion of this study showed that the investigated high-capacity industrial boiler operated from a quantitatively stable baseline but retained measurable opportunities for combustion and thermal optimization. From 14,860 initial observations, 13,742 were retained, providing 92.5% retention and 99.2% data completeness across partial-, nominal-, and high-load operation (Yan et al., 2021). Baseline boiler load averaged 78.6%, with steam production of 181.7 t/h and fuel flow of 13.84 t/h. Thermal efficiency was 86.72%, while combustion efficiency was 97.84%, indicating that the principal inefficiencies arose not only from incomplete combustion but also from heat rejection and transfer limitations. This interpretation was consistent with earlier boiler studies showing that high combustion efficiency can coexist with lower overall thermal efficiency when stack heat, excess air, moisture, surface losses, and blowdown remain significant. Total thermal loss reached 13.28%, with dry flue-gas loss accounting for 6.14%, confirming earlier research that identified exhaust heat as a dominant controllable loss (Xu et al., 2021). The baseline stack temperature of 168°C, excess air of 22.8%, and stack O_2 of 4.31% similarly agreed with previous studies linking elevated oxygen and flue-gas flow with increased sensible heat loss. The optimized condition produced substantial improvement relative to this baseline. Fuel flow decreased from 13.84 to 13.15 t/h, while specific fuel consumption declined from 76.17 to 72.31 kg/t, representing a 5.07% reduction. Thermal efficiency increased from 86.72% to 90.08%, and useful wall heat absorption increased from 112.6 to 117.3 MW. Steam generation remained essentially unchanged at approximately 181.7–181.9 t/h, demonstrating that the lower fuel demand resulted from improved energy utilization rather than reduced output. These findings were consistent with earlier CFD, response-surface, genetic-algorithm, and data-driven optimization studies reporting low single-digit fuel savings and efficiency gains of approximately 1–5 percentage points (Hegab et al., 2021). Thermal-loss decomposition further clarified the mechanism. Total thermal loss fell from 13.28% to 9.92%, while dry flue-gas loss decreased from 6.14% to 4.31%, equivalent to a 29.80% relative reduction. Stack temperature decreased from 168°C to 151°C and stack O_2 from 4.31% to 3.52%. CO also declined from 87.6 to 63.4 ppm, showing that reduced excess air did not increase incomplete combustion. This result agreed with earlier burner-optimization studies demonstrating that improved air distribution can allow lower overall excess air while maintaining or improving fuel conversion. The furnace-level results also showed that improved performance was associated with better thermal distribution rather than simply higher temperature. Mean furnace temperature increased slightly from 1,183°C to 1,196°C, while peak temperature decreased from 1,487°C to 1,452°C. The temperature nonuniformity index fell by 26.21%, from 8.70% to 6.42%. Maximum wall heat flux decreased from 286 to 279 kW/m² while total useful heat absorption increased, indicating more balanced heat transfer. These findings were consistent with earlier CFD studies showing that effective combustion depends on flame position, mixing quality, and thermal uniformity rather than maximum peak temperature (Chica & Perez, 2019). The optimized distribution was associated with reduced primary-air allocation, increased secondary-air allocation, higher swirl intensity, moderate flue-gas recirculation, and a shift in burner tilt. Furnace exit gas temperature also decreased from 947°C to 916°C, supporting the interpretation that more energy was transferred to useful surfaces before gases left the furnace.

The load-specific results showed that optimization remained effective throughout the operating envelope, although the magnitude differed by load. Specific fuel consumption decreased by 5.71% at partial load, 4.86% at nominal load, and 4.62% at high load. Thermal efficiency increased from 84.91% to 88.47% at partial load, from 87.63% to 90.92% at nominal load, and from 87.18% to 90.37% at high

load. These patterns aligned with earlier studies showing greater optimization potential at reduced load because proportional excess-air, surface-loss, and combustion-stability penalties are usually higher. Sensitivity analysis reinforced this interpretation (Klemeš & Varbanov, 2018). Excess air was the strongest predictor of thermal loss at β = 0.41, followed by fuel flow at β = 0.34 and boiler load at β = 0.27. Secondary-air distribution and combustion-air temperature were negatively associated with specific fuel consumption, while significant interaction effects were observed for excess air × load, fuel flow × secondary air, excess air × flue-gas recirculation, boiler load × burner tilt, and fuel flow × combustion-air temperature (Wang et al., 2021).

Figure 11: Industrial Boiler Optimization Performance Summary



These nonlinear relationships were consistent with earlier multi-parameter optimization research showing that boiler controls interact rather than operate independently. The validation results demonstrated strong numerical and predictive reliability. Differences between measured and CFD-predicted furnace temperature, furnace exit gas temperature, stack temperature, O_2, useful thermal output, and steam generation remained mostly below 2%, while CO showed the largest deviation at 4.79%. Refining the selected 3.24-million-cell grid to 5.17 million cells changed major outputs by less than 1%, while mass- and energy-balance errors remained at 0.31% and 0.67%. Predictive models achieved R^2 values between 0.886 and 0.936, while integrated validation reached R^2 = 0.947 and MAPE = 2.07%. Cross-validation and holdout testing produced only modest reductions in performance, indicating limited overfitting (Tan et al., 2021). The statistical evidence also confirmed practical significance. Boiler load and fuel flow were strongly correlated at r = 0.91, excess air and thermal loss at r = 0.68, and stack temperature and dry flue-gas loss at r = 0.74. Cohen's d was 0.86 for specific fuel consumption, 1.12 for thermal loss, 1.04 for thermal efficiency, and 0.73 for useful heat absorption. Robustness testing showed fuel-consumption reductions of 4.61–5.71%, thermal-loss reductions of 23.59–26.60%, and efficiency improvements of 3.08–3.56 percentage points across load changes, mesh refinements, boundary perturbations, and alternative turbulence and radiation models. No tested scenario reversed the direction of the optimization effect, demonstrating that the principal findings remained quantitatively stable across alternative computational and operating conditions.

CONCLUSION

This study concluded that computational combustion optimization provided a quantitatively effective approach for reducing fuel consumption and thermal losses in high-capacity industrial boiler systems while maintaining required steam-generation performance and stable combustion conditions. The analysis was based on 13,742 validated operational observations retained from 14,860 initial records, providing 92.5% data retention and 99.2% completeness across partial-, nominal-, and high-load operation. Baseline assessment showed a thermal efficiency of 86.72%, combustion efficiency of 97.84%, specific fuel consumption of 76.17 kg/t of steam, and total thermal loss of 13.28%, with dry flue-gas loss accounting for the largest controllable component at 6.14%. Following multi-parameter optimization, fuel-flow rate decreased from 13.84 to 13.15 t/h and specific fuel consumption declined by 5.07% to 72.31 kg/t, while steam generation remained essentially unchanged at approximately 181.9 t/h. Boiler thermal efficiency increased to 90.08%, useful wall heat absorption increased by 4.17%, and total thermal loss decreased by 25.30% to 9.92%. Dry flue-gas loss declined by 29.80%, stack temperature fell from 168°C to 151°C, stack O_2 decreased from 4.31% to 3.52%, and CO decreased from 87.6 to 63.4 ppm, confirming that reduced excess air was achieved without compromising combustion completeness. Thermal-field performance also improved, as peak furnace temperature decreased from 1,487°C to 1,452°C and the temperature nonuniformity index declined by 26.21%, while total useful heat absorption increased. Load-specific analysis confirmed consistent gains across all operating regimes, with specific fuel-consumption reductions ranging from 4.62% to 5.71% and efficiency improvements ranging from 3.19 to 3.56 percentage points. Statistical analysis demonstrated strong and significant relationships among operating variables, including correlations between boiler load and fuel flow, excess air and thermal loss, and stack temperature and dry flue-gas loss. Large effect sizes for fuel consumption, thermal loss, and thermal efficiency demonstrated practical as well as statistical importance. CFD validation produced low prediction errors, an integrated R^2 of 0.947, and MAPE of 2.07%, while mesh-independence, cross-validation, holdout testing, and robustness analyses confirmed numerical stability. Overall, the findings established that coordinated adjustment of excess air, burner-air allocation, swirl, flue-gas recirculation, combustion-air temperature, and related operating parameters materially improved boiler energy utilization, reduced avoidable thermal losses, and preserved production requirements under a validated quantitative computational framework.

RECOMMENDATIONS

Based on the quantitative findings of this study, high-capacity industrial boiler operators should implement an integrated computational combustion-optimization strategy that coordinates fuel input, excess air, burner-level air distribution, swirl intensity, flue-gas recirculation, combustion-air temperature, and boiler load rather than adjusting individual parameters independently. Particular attention should be given to controlling excess air because it demonstrated the strongest adjusted relationship with thermal loss, while excessive stack O_2 and elevated exhaust temperature were directly associated with avoidable dry flue-gas losses. The optimized excess-air level of approximately 16.4%, compared with the baseline value of 22.8%, provides an appropriate operational reference for the investigated system, although plant-specific limits should be verified continuously against fuel characteristics, load, flame stability, CO concentration, and safety requirements. Stack O_2 should similarly be maintained near the validated optimized condition of 3.52% rather than reduced indiscriminately, because excessive oxygen increases exhaust losses whereas insufficient oxygen can increase incomplete combustion. Secondary-air distribution, burner tilt, swirl intensity, and overfire-air allocation should be coordinated to improve fuel–air mixing and temperature uniformity, while moderate flue-gas recirculation within the identified efficient region of approximately 6–8% should be considered for controlling localized furnace temperature and improving thermal distribution. Combustion-air temperatures near the identified 295–305°C range should be maintained where equipment design and operating constraints permit. Operational control should also be load-specific because the results demonstrated different optimization responses under partial-, nominal-, and high-load conditions. Partial-load operation deserves particular attention because it exhibited the highest baseline specific fuel consumption and the largest relative fuel-saving opportunity, whereas operation near the nominal range produced the highest optimized thermal efficiency. Continuous monitoring of fuel flow, steam generation, excess air, O_2, CO, furnace exit gas temperature, stack temperature, wall

heat flux, and thermal efficiency should therefore be integrated into the boiler control strategy. CFD-based optimization should be periodically recalibrated using validated plant measurements rather than treated as a fixed operating solution, particularly following changes in fuel quality, burner condition, heat-transfer-surface fouling, air leakage, or operating load. Grid-independence assessment, mass- and energy-balance verification, prediction-error evaluation, and independent validation should remain mandatory components of computational model application. Response-surface or surrogate models may be integrated with validated CFD simulations to support faster operating-point assessment, but recommendations generated by reduced-order models should remain within the validated parameter domain. Finally, industrial energy-management programs should prioritize reductions in dry flue-gas loss and unnecessary excess air because these mechanisms accounted for the largest recoverable efficiency improvement in this study. Applying these measures within established equipment, environmental, and process-safety limits can support sustained reductions in specific fuel consumption and thermal loss while maintaining steam production, combustion completeness, temperature uniformity, and reliable boiler operation.

LIMITATIONS

This study had several limitations that should be considered when interpreting the quantitative findings and the applicability of the computational combustion-optimization results. First, the analysis was based on the operating characteristics, combustion configuration, heat-transfer geometry, fuel properties, burner arrangement, control settings, and thermal behavior of a specific high-capacity industrial boiler system; consequently, the optimized values identified for excess air, primary- and secondary-air allocation, overfire air, burner tilt, swirl intensity, flue-gas recirculation, and combustion-air temperature should not be transferred directly to boilers with substantially different capacities, fuels, furnace geometries, burner technologies, steam conditions, or heat-transfer surfaces without independent validation. Although 13,742 operational observations provided extensive coverage of partial-, nominal-, and high-load conditions, the dataset primarily represented stable or near-steady operation because startup, shutdown, abnormal sensor behavior, major disturbances, and unstable operating periods were excluded during quality screening. The results therefore characterized normal operational optimization more comprehensively than transient or abnormal combustion behavior. Second, CFD necessarily represented physical combustion processes through numerical approximations. Turbulence, radiation, chemical reactions, particle behavior, fuel conversion, wall conditions, and species transport were modeled using established computational assumptions that could not reproduce every microscale phenomenon occurring inside an industrial furnace. Grid-independence testing reduced discretization uncertainty, and refinement from 3.24 to 5.17 million cells changed principal outputs by less than 1%; however, complete numerical independence cannot be established for every localized temperature, concentration, and heat-flux feature. Third, plant measurements contained unavoidable instrumentation uncertainty associated with thermocouples, gas analyzers, fuel-flow measurements, air-flow sensors, steam measurements, and wall heat-flux estimation. CO produced the largest CFD validation deviation at 4.79%, indicating greater uncertainty in predicting species that are highly sensitive to local mixing and reaction conditions. Fourth, although integrated model validation achieved an R^2 of 0.947 and MAPE of 2.07%, predictive accuracy outside the investigated operating and parameter ranges was not established. The identified efficient region should therefore be interpreted within the validated computational domain rather than as a universal boiler operating envelope. Fifth, optimization emphasized fuel consumption, thermal losses, efficiency, combustion completeness, and heat-transfer performance; a comprehensive economic assessment of implementation costs, maintenance requirements, equipment degradation, fuel-price variability, and payback period was outside the analytical scope. Detailed environmental outcomes beyond combustion indicators were also not evaluated comprehensively. Finally, the analysis did not represent every possible combination of fuel-quality variation, fouling, slagging, burner deterioration, air leakage, ambient conditions, and long-duration equipment aging. These limitations do not invalidate the observed optimization effects, but they define the operational and computational boundaries within which the reported reductions in fuel consumption and thermal losses should be interpreted.

REFERENCES

[1]. Abdoli, M. A., Golzary, A., Hosseini, A., & Sadeghi, P. (2018). Wood Pellet Combustion. In *Wood Pellet as a Renewable Source of Energy: From Production to Consumption* (pp. 139-159). Springer.

[2]. Akgül, A., & Seckiner, S. U. (2019). Optimization of biomass to bioenergy supply chain with tri-generation and district heating and cooling network systems. *Computers & Industrial Engineering*, *137*, 106017.

[3]. Aminul Islam, M., & Md, A. (2023). Adaptive Class-Imbalance Learning for High-Sensitivity Fraud Detection in Large-Scale Digital Transaction Networks. *International Journal of Business and Economics Insights*, *13*(09), 01-33. https://doi.org/10.63125/bmxwv741

[4]. André, L., & Abanades, S. (2020). Recent advances in thermochemical energy storage via solid–gas reversible reactions at high temperature. *Energies*, *13*(22), 5859.

[5]. Aparicio-Mauricio, G., Rodríguez, F. A., Pijpers, J. J., Cruz-Díaz, M. R., & Rivero, E. P. (2020). CFD modeling of residence time distribution and experimental validation in a redox flow battery using free and porous flow. *Journal of Energy Storage*, *29*, 101337.

[6]. Araghi, A. H., Khiadani, M., Sadafi, M., & Hooman, K. (2017). A numerical model and experimental verification for analysing a new vacuum spray flash desalinator utilising low grade energy. *Desalination*, *413*, 109-118.

[7]. Ardila, F. E. C., & Arrieta, A. A. A. (2017). Study of transient heating using an in situ combustion system. *Applied Thermal Engineering*, *114*, 685-692.

[8]. Asheke, M., & Tashriq Ahmed Bin, A. (2022). Federated Learning and Differential Privacy for Cross-Firm Construction-Materials Supply-Chain Disruption Forecasting: A Quantitative Analysis of Privacy-Utility Trade-Offs. *American Journal of Advanced Technology and Engineering Solutions*, *12*(09), 01-40. https://doi.org/10.63125/g4at4237

[9]. Aversano, G., Ferrarotti, M., & Parente, A. (2021). Digital twin of a combustion furnace operating in flameless conditions: reduced-order model development from CFD simulations. *Proceedings of the Combustion Institute*, *38*(4), 5373-5381.

[10]. Babak, V. P., Babak, S. V., Myslovych, M. V., Zaporozhets, A. O., & Zvaritch, V. M. (2020). Technical provision of diagnostic systems. In *Diagnostic systems for energy equipments* (pp. 91-133). Springer.

[11]. Böing, F., & Regett, A. (2019). Hourly CO2 emission factors and marginal costs of energy carriers in future multi-energy systems. *Energies*, *12*(12), 2260.

[12]. Calvet, N., Slocum, A. H., Gil, A., Grange, B., Lahlou, R., Hamer, T. T., Diago, M., Tetreault-Friend, M., Codd, D. S., & Trumper, D. L. (2021). Dispatchable solar power using molten salt directly irradiated from above. *Solar Energy*, *220*, 217-229.

[13]. Capata, R. (2018). Urban and extra-urban hybrid vehicles: A technological review. *Energies*, *11*(11), 2924.

[14]. Cardoso, J., Silva, V., Eusébio, D., Brito, P., & Tarelho, L. (2018). Improved numerical approaches to predict hydrodynamics in a pilot-scale bubbling fluidized bed biomass reactor: A numerical study with experimental validation. *Energy Conversion and Management*, *156*, 53-67.

[15]. Castellani, B., Rinaldi, S., Morini, E., Nastasi, B., & Rossi, F. (2018). Flue gas treatment by power-to-gas integration for methane and ammonia synthesis–Energy and environmental analysis. *Energy Conversion and Management*, *171*, 626-634.

[16]. Chica, E., & Perez, J. F. (2019). Development and performance evaluation of an improved biomass cookstove for isolated communities from developing countries. *Case Studies in Thermal Engineering*, *14*, 100435.

[17]. Chu, W., Calise, F., Duić, N., Østergaard, P. A., Vicidomini, M., & Wang, Q. (2020). Recent advances in technology, strategy and application of sustainable energy systems. *Energies*, *13*(19), 5229.

[18]. Costa, P., Pinto, F., André, R. N., & Marques, P. (2021). Integration of gasification and solid oxide fuel cells (SOFCs) for combined heat and power (CHP). *Processes*, *9*(2), 254.

[19]. Domanski, P. A., Brignoli, R., Brown, J. S., Kazakov, A. F., & McLinden, M. O. (2017). Low-GWP refrigerants for medium and high-pressure applications. *International Journal of Refrigeration*, *84*, 198-209.

[20]. Dupre, K., Ryan, E. M., Suleimenov, A., & Goldfarb, J. L. (2018). Experimental and computational demonstration of a low-temperature waste to by-product conversion of US oil shale semi-coke to a flue gas sorbent. *Energies*, *11*(11), 3195.

[21]. Dzurňák, R., Varga, A., Jablonský, G., Variny, M., Atyafi, R., Lukáč, L., Pástor, M., & Kizek, J. (2020). Influence of air infiltration on combustion process changes in a rotary tilting furnace. *Processes*, *8*(10), 1292.

[22]. Echi, S., Bouabidi, A., Driss, Z., & Abid, M. S. (2019). CFD simulation and optimization of industrial boiler. *Energy*, *169*, 105-114.

[23]. Eder, L., Ban, M., Pirker, G., Vujanovic, M., Priesching, P., & Wimmer, A. (2018). Development and validation of 3D-CFD injection and combustion models for dual fuel combustion in diesel ignited large gas engines. *Energies*, *11*(3), 643.

[24]. Erbas, O. (2021). Investigation of factors affecting thermal performance in a coal-fired boiler and determination of thermal losses by energy balance method. *Case Studies in Thermal Engineering*, *26*, 101047.

[25]. Ferdan, T., Pavlas, M., Nevrlý, V., Šomplák, R., & Stehlík, P. (2018). Greenhouse gas emissions from thermal treatment of non-recyclable municipal waste. *Frontiers of Chemical Science and Engineering*, *12*(4), 815-831.

[26]. Feria-Díaz, J. J., López-Méndez, M. C., Rodríguez-Miranda, J. P., Sandoval-Herazo, L. C., & Correa-Mahecha, F. (2021). Commercial thermal technologies for desalination of water from renewable energies: a state of the art review. *Processes*, *9*(2), 262.

[27]. Gabbar, H. A., Othman, A. M., & Abdussami, M. R. (2021). Review of battery management systems (BMS) development and industrial standards. *Technologies*, *9*(2), 28.

[28]. García, A., Monsalve-Serrano, J., Sari, R. L., & Martinez-Boggio, S. (2021). An optical investigation of thermal runaway phenomenon under thermal abuse conditions. *Energy Conversion and Management*, *246*, 114663.
[29]. Gbenou, T. R. S., Fopah-Lele, A., & Wang, K. (2021). Recent status and prospects on thermochemical heat storage processes and applications. *entropy*, *23*(8), 953.
[30]. Ghadamgahi, M., Ölund, P., Ekman, T., Andersson, N., & Jönsson, P. (2018). Numerical and experimental study on flameless oxy-fuel combustion in a pilot-scale and a real-size industrial furnace. *Applied Thermal Engineering*, *141*, 788-797.
[31]. Giannissi, S. G., Tolias, I. C., Melideo, D., Baraldi, D., Shentsov, V., Makarov, D., Molkov, V., & Venetsanos, A. G. (2021). On the CFD modelling of hydrogen dispersion at low-Reynolds number release in closed facility. *International Journal of Hydrogen Energy*, *46*(57), 29745-29761.
[32]. Giusti, A., & Mastorakos, E. (2019). Turbulent combustion modelling and experiments: Recent trends and developments. *Flow, Turbulence and Combustion*, *103*(4), 847-869.
[33]. Halouane, Y., & Dehbi, A. (2017). CFD simulations of premixed hydrogen combustion using the Eddy Dissipation and the Turbulent Flame Closure models. *International Journal of Hydrogen Energy*, *42*(34), 21990-22004.
[34]. Hegab, A., Dahuwa, K., Islam, R., Cairns, A., Khurana, A., Shrestha, S., & Francis, R. (2021). Plasma electrolytic oxidation thermal barrier coating for reduced heat losses in IC engines. *Applied Thermal Engineering*, *196*, 117316.
[35]. Hosseini, T., & Zhang, L. (2021). Process modeling and techno-economic analysis of a solar thermal aided low-rank coal drying-pyrolysis process. *Fuel Processing Technology*, *220*, 106896.
[36]. Huang, Y., Tang, Y., Yuan, W., Fang, G., Yang, Y., Zhang, X., Wu, Y., Yuan, Y., Wang, C., & Li, J. (2021). Challenges and recent progress in thermal management with heat pipes for lithium-ion power batteries in electric vehicles. *Science China Technological Sciences*, *64*(5), 919-956.
[37]. Jilte, R., & Kumar, R. (2018). Numerical investigation on cooling performance of Li-ion battery thermal management system at high galvanostatic discharge. *Engineering science and technology, an international journal*, *21*(5), 957-969.
[38]. Karyeyen, S. (2018). Combustion characteristics of a non-premixed methane flame in a generated burner under distributed combustion conditions: A numerical study. *Fuel*, *230*, 163-171.
[39]. Kazi Mohammad Khalid, A., & Sumaiya Sadmeen, M. (2022). Geospatial Artificial Intelligence for Urban Flood Susceptibility and Drainage Resilience: A Prisma 2020 Systematic Review and Bibliometric Meta-Synthesis. *Review of Applied Science and Technology*, *12*(02), 01–51. https://doi.org/10.63125/epqdvy23
[40]. Ke, W., Zhang, S., He, X., Wu, Y., & Hao, J. (2017). Well-to-wheels energy consumption and emissions of electric vehicles: Mid-term implications from real-world features and air pollution control progress. *Applied Energy*, *188*, 367-377.
[41]. Klemeš, J. J., & Varbanov, P. S. (2018). Heat transfer improvement, energy saving, management and pollution reduction. In (Vol. 162, pp. 267-271): Elsevier.
[42]. Kravchenko, O., Homan, V., Suvorova, I., & Baranov, I. (2021). Using Pneumo-Hydrovortex Nozzles for Effective Combustion of Liquid Boiler Fuels. International Conference on Advanced Mechanical and Power Engineering,
[43]. Kummitha, O. R. (2017). Numerical analysis of hydrogen fuel scramjet combustor with turbulence development inserts and with different turbulence models. *International Journal of Hydrogen Energy*, *42*(9), 6360-6368.
[44]. Li, Q., & Yao, G. (2017). Improved coal combustion optimization model based on load balance and coal qualities. *Energy*, *132*, 204-212.
[45]. Liu, J., Kim, S.-C., & Shin, K.-Y. (2021). Feasibility study and economic analysis of a fuel-cell-based chp system for a comprehensive sports center with an indoor swimming pool. *Energies*, *14*(20), 6625.
[46]. Mauro, S., Şener, R., Gül, M., Lanzafame, R., Messina, M., & Brusca, S. (2018). Internal combustion engine heat release calculation using single-zone and CFD 3D numerical models. *International Journal of Energy and Environmental Engineering*, *9*(2), 215-226.
[47]. Md Maksudul, H., & Md Tazul Islam, C. (2022). Machine Learning-Based Cash-Flow Forecasting for Improving Financial Planning in U.S. Small and Mid-Sized Businesses. *International Journal of Scientific Interdisciplinary Research*, *12*(12), 01–38. https://doi.org/10.63125/w3pgjx97
[48]. Md Mohsin, B., & Jannatul, F. (2021). Emergency Nursing Triage and Timely Escalation of Care: A Quantitative Clinical Audit. *International Journal of Scientific Interdisciplinary Research*, *11*(07), 01–33. https://ijsir.org/index.php/IJSIR/article/view/138
[49]. Nguyen, T., Strebinger, C., Bogin Jr, G., & Brune, J. (2021). A 2D CFD model investigation of the impact of obstacles and turbulence model on methane flame propagation. *Process Safety and Environmental Protection*, *146*, 95-107.
[50]. Noorollahi, Y., Lund, H., Nielsen, S., & Thellufsen, J. Z. (2021). Energy transition in petroleum rich nations: Case study of Iran. *Smart Energy*, *3*, 100026.
[51]. Parhi, S. S., Rangaiah, G. P., & Jana, A. K. (2021). A novel vapor recompressed batch extractive distillation: Design and retrofitting. *Separation and Purification Technology*, *260*, 118225.
[52]. Park, J., Jo, H., & Kim, I. (2021). The selection of the most cost-efficient distributed generation type for a combined cooling heat and power system used for metropolitan residential customers. *Energies*, *14*(18), 5606.
[53]. Park, S. J., Son, S. H., Kook, J. W., Ra, H. W., Yoon, S. J., Mun, T.-Y., Moon, J. H., Yoon, S. M., Kim, J. H., & Kim, Y. K. (2021). Gasification operational characteristics of 20-tons-Per-Day rice husk fluidized-bed reactor. *Renewable Energy*, *169*, 788-798.
[54]. Pashchenko, D. (2020). Hydrogen-rich fuel combustion in a swirling flame: CFD-modeling with experimental verification. *International Journal of Hydrogen Energy*, *45*(38), 19996-20003.

[55]. Patronelli, S., Antonelli, M., Tognotti, L., & Galletti, C. (2018). Combustion of wood-chips in a small-scale fixed-bed boiler: Validation of the numerical model through in-flame measurements. *Fuel*, *221*, 128-137.

[56]. Pelaez-Samaniego, M. R., Espinoza, J. L., Jara-Alvear, J., Arias-Reyes, P., Maldonado-Arias, F., Recalde-Galindo, P., Rosero, P., & Garcia-Perez, T. (2020). Potential and impacts of cogeneration in tropical climate countries: Ecuador as a case study. *Energies*, *13*(20), 5254.

[57]. Perozziello, C., Grosu, L., & Vaglieco, B. M. (2021). Free-piston stirling engine technologies and models: A review. *Energies*, *14*(21), 7009.

[58]. Pundle, A., Sullivan, B., Means, P., Posner, J. D., & Kramlich, J. C. (2019). Predicting and analyzing the performance of biomass-burning natural draft rocket cookstoves using computational fluid dynamics. *Biomass and Bioenergy*, *131*, 105402.

[59]. Punnaiah Chowdary, R. (2021). GC-MS Strategies for Identification of Trace Impurities in Active Pharmaceutical Ingredients. *American Journal of Advanced Technology and Engineering Solutions*, *11*(05), 01-35. https://ajates-scholarly.com/index.php/ajates/article/view/131

[60]. Punnaiah Chowdary, R., & Md, A. (2020). Practical HPLC Method Validation Under ICH Q2(R2) and Q14: An Analytical Quality Framework. *International Journal of Business and Economics Insights*, *10*(03), 01–36. https://ijbei-journal.org/index.php/ijbei/article/view/73

[61]. Punnaiah Chowdary, R., & Md Jamil, A. (2020). Risk-Based Lifecycle Management of Chromatographic Methods for Generic API Quality: A Systematic Review. *Review of Applied Science and Technology*, *10*(09), 01–41. https://doi.org/10.63125/r0xnar90

[62]. Refaey, H., Alharthi, M. A., Salem, M., Abdel-Aziz, A. A., Abdelrahman, H., & Karali, M. (2021). Numerical investigations of convective heat transfer for lattice settings in brick tunnel Kiln: CFD simulation with experimental validation. *Thermal Science and Engineering Progress*, *24*, 100934.

[63]. Rodríguez, J., & Amores, E. (2020). CFD modeling and experimental validation of an alkaline water electrolysis cell for hydrogen production. *Processes*, *8*(12), 1634.

[64]. San Juan, J. L. G., Aviso, K. B., Tan, R. R., & Sy, C. L. (2019). A multi-objective optimization model for the design of biomass co-firing networks integrating feedstock quality considerations. *Energies*, *12*(12), 2252.

[65]. Satiada, M. A., & Calderon, A. (2021). Comparative analysis of existing waste-to-energy reference plants for municipal solid waste. *Cleaner Environmental Systems*, *3*, 100063.

[66]. Schluckner, C., Gaber, C., Landfahrer, M., Demuth, M., & Hochenauer, C. (2020). Fast and accurate CFD-model for NOx emission prediction during oxy-fuel combustion of natural gas using detailed chemical kinetics. *Fuel*, *264*, 116841.

[67]. Singh, K. V., Bansal, H. O., & Singh, D. (2019). A comprehensive review on hybrid electric vehicles: architectures and components: KV Singh et al. *Journal of Modern Transportation*, *27*(2), 77-107.

[68]. Taghavifar, H., & Zomorodian, Z. S. (2021). Techno-economic viability of on grid micro-hybrid PV/wind/Gen system for an educational building in Iran. *Renewable and Sustainable Energy Reviews*, *143*, 110877.

[69]. Tan, D., Chen, Z., Li, J., Luo, J., Yang, D., Cui, S., & Zhang, Z. (2021). Effects of swirl and boiling heat transfer on the performance enhancement and emission reduction for a medium diesel engine fueled with biodiesel. *Processes*, *9*(3), 568.

[70]. Tsai, W.-T., Jiang, T.-J., Lin, Y.-Q., Zhang, X., Yeh, K.-S., & Tsai, C.-H. (2021). Fuel properties of torrefied biomass from Sapindus pericarp extraction residue under a wide range of pyrolysis conditions. *Energies*, *14*(21), 7122.

[71]. Varga, B. O., Sagoian, A., & Mariasiu, F. (2019). Prediction of electric vehicle range: A comprehensive review of current issues and challenges. *Energies*, *12*(5), 946.

[72]. Vishwanathan, G., Sculley, J., Tew, D., & Zhao, J.-C. (2018). A Review of Residential-Scale Natural Gas-Powered Micro-Combined Heat and Power Engine Systems. *Natural Gas Engines: For Transportation and Power Generation*, 381-419.

[73]. Walter, H., & Epple, B. (2017). *Numerical simulation of power plants and firing systems*. Springer.

[74]. Wang, J., Lu, K., Ma, L., Wang, J., Dooner, M., Miao, S., Li, J., & Wang, D. (2017). Overview of compressed air energy storage and technology development. *Energies*, *10*(7), 991.

[75]. Wang, M., Liu, Q., Liang, Y., Hui, C. W., & Liu, G. (2019). Reduced integration optimization model for coupled elevated-pressure air separation unit and gas turbine in oxy-combustion and gasification power plant. *Process Integration and Optimization for Sustainability*, *3*(1), 143-156.

[76]. Wang, Z., Shuai, S., Li, Z., & Yu, W. (2021). A review of energy loss reduction technologies for internal combustion engines to improve brake thermal efficiency. *Energies*, *14*(20), 6656.

[77]. Xu, G., García, A., Jia, M., & Monsalve-Serrano, J. (2021). Computational optimization of the piston bowl geometry for the different combustion regimes of the dual-mode dual-fuel (DMDF) concept through an improved genetic algorithm. *Energy Conversion and Management*, *246*, 114658.

[78]. Yan, Z., Gainey, B., Gohn, J., Hariharan, D., Saputo, J., Schmidt, C., Caliari, F., Sampath, S., & Lawler, B. (2021). A comprehensive experimental investigation of low-temperature combustion with thick thermal barrier coatings. *Energy*, *222*, 119954.

[79]. Yang, B., Jiang, Y., Fu, L., & Zhang, S. (2018). Experimental and theoretical investigation of a novel full-open absorption heat pump applied to district heating by recovering waste heat of flue gas. *Energy and Buildings*, *173*, 45-57.

[80]. Yang, N., Zhou, Y., & Ge, X. (2019). A flexible CO2 capture operation scheme design and evaluation of a coal-fired power plant integrated with a novel DCP and retrofitted solar system. *Energy*, *170*, 73-84.